One-sentence summary: Sensory neurons expressing the GPCR Mrgprd mediate the effects of a bioactive lipid to cause abdominal pain.

Editor's summary:
Inducing pain in IBS
A symptom of irritable bowel syndrome (IBS) that accompanies altered bowel function is abdominal pain. Noting that various polyunsaturated fatty acids (PUFAs) are implicated in modulating inflammation in patients with IBS, Bautzova *et al*. found that the abundance of the PUFA 5-oxoETE was selectively increased in colonic biopsies from patients with a subtype of IBS characterized by constipation (IBS-C). 5-oxoETE increased pain sensitivity in mice without eliciting inflammation and stimulated both mouse and human dorsal root ganglia neurons expressing the GPCR Mrgprd. Knockdown of Mrgprd in mice reduced the percentage of neurons that responded to 5-oxoETE and decreased pain sensitivity, suggesting that this PUFA may mediate abdominal pain in patients with IBS-C.

5-oxoETE triggers nociception in constipation-predominant irritable bowel syndrome through MAS-related G protein–coupled receptor D

Tereza Bautzova[1*], James R. F. Hockley[2,3*], Teresa Perez-Berezo[1*], Julien Pujo[1], Michael M. Tranter[3], Cleo Desormeaux[1], Maria Raffaella Barbaro[4], Lilian Basso[1†], Pauline Le Faouder[5], Corinne Rolland[1], Pascale Malapert[6], Aziz Moqrich[6], Helene Eutamene[7], Alexandre Denadai-Souza[1§], Nathalie Vergnolle[1,8], Ewan St John Smith[2], David I. Hughes[9], Giovanni Barbara[4], Gilles Dietrich[1], David C. Bulmer[2,3], Nicolas Cenac[1‡]

[1]INSERM, UMR1220, IRSD, Université de Toulouse, INRA, ENVT, UPS, Toulouse, France. [2]Department of Pharmacology, University of Cambridge, Tennis Court Road, Cambridge CB1 2PD, UK. [3]National Centre for Bowel Research and Surgical Innovation, Blizard Institute, Barts and the London School of Medicine and Dentistry, Queen Mary University of London, London E1 2AJ, UK. [4]Department of Medical and Surgical Sciences, University of Bologna, Bologna, Italy. [5]INSERM UMR1048, Lipidomic Core Facility, Metatoul Platform, Université de Toulouse, Toulouse, France. [6]Aix-Marseille-Université, CNRS, Institut de Biologie du Développement de Marseille, UMR 7288, Marseille, France. [7]Neuro-Gastroenterology and Nutrition Team, UMR 1331, INRA Toxalim, INP-EI-Purpan, Université de Toulouse, Toulouse, France. [8]Departments of Physiology & Pharmacology, and Medicine, University of Calgary Cumming School of Medicine, 3330 Hospital Drive NW, Calgary, Alberta, T2N 4N1, Canada. [9]Institute of Neuroscience and Psychology, University of Glasgow, Glasgow, UK.

[*]These authors contributed equally to this work.

[†]Current address: Snyder Institute for Chronic Diseases, Cumming School of Medicine, University of Calgary, 3330 Hospital Drive N.W., Calgary, Alberta, Canada, T2N 4N1.

[§]Current address: Department of Chronic Diseases, Metabolism and Ageing; Translational Research Center for Gastrointestinal Disorders, Laboratory for Intestinal Neuroimmune Interactions, KU Leuven, Leuven, Belgium.

[‡]Corresponding author. Email: nicolas.cenac@inserm.fr

Abstract

Irritable bowel syndrome (IBS) is a common gastrointestinal disorder that is characterized by chronic abdominal pain concurrent with altered bowel habit. Polyunsaturated fatty acid (PUFA) metabolites are increased in abundance in IBS and are implicated in the alteration of sensation to mechanical stimuli, which is defined as visceral hypersensitivity. We sought to quantify PUFA metabolites in IBS patients and evaluate their role in pain. Quantification of PUFA metabolites by mass spectrometry in colonic biopsies showed an increased abundance of 5-oxo-eicosatetraenoic acid (5-oxoETE) only in biopsies taken from patients with IBS with predominant constipation (IBS-C). Local administration of 5-oxoETE to mice induced somatic and visceral hypersensitivity to mechanical stimuli without causing tissue inflammation. We found that 5-oxoETE directly acted on both human and mouse sensory neurons as shown by lumbar splanchnic nerve recordings and Ca^{2+}-imaging of dorsal root ganglia (DRG) neurons. We showed that 5-oxoETE selectively stimulated nonpeptidergic, isolectin B4 (IB4)-positive DRG neurons through a phospholipase C (PLC)– and pertussis toxin–dependent mechanism, suggesting that the effect was mediated by a G protein–coupled receptor (GPCR). The MAS-related GPCR D (Mrgprd) was found in mouse colonic DRG afferents and was identified as being implicated in the noxious effects of 5-oxoETE. Together, these data suggest that 5-oxoETE, a potential biomarker of IBS-C, induces somatic and visceral hyperalgesia without inflammation in an Mrgprd-dependent manner. Thus, 5-oxoETE may play a pivotal role in the abdominal pain associated with IBS-C.

Introduction

Irritable bowel syndrome (IBS) is a functional bowel disorder in which recurrent abdominal pain is associated with a change in bowel habit, typically constipation (IBS-C), diarrhea (IBS-D), or a mixed (constipation and diarrhea) bowel habit (IBS-M) (1). IBS is a common disorder in Western populations, which affects around 11% of the global population (*2*), with a higher prevalence in women than in men (1). Although the aetiology of IBS remains unclear, low-grade inflammation has been widely described in this disorder, with several fundamental studies implicating proinflammatory molecules in the pathophysiology of IBS symptoms (*3*). We previously showed that the amounts of several polyunsaturated fatty acid (PUFA) metabolites, also defined as bioactive lipids, are statistically significantly altered in biopsy samples from patients with IBS compared to those in samples from healthy controls (*4*). This is in agreement with previous studies focused on the prostanoid subtype of PUFA metabolites (*5*-*7*).

The functional relationship between PUFAs and pain has been the subject of many studies (*8*). Both basic and clinical studies have revealed that a dietary intake of n-3 series PUFAs results in a reduction in pain associated with rheumatoid arthritis (*9, 10*), dysmenorrhea (*11*), inflammatory bowel disease (*12*), and neuropathy (*13*), whereas n-6 series PUFAs are high in abundance in patients with chronic pain, including IBS patients (*4, 14, 15*). The n-3 PUFA metabolites, such as resolvins (Rvs), are analgesic in multiple pain models, an effect attributed to inhibition of certain transient receptor potential (TRP) channels (*16*). For example, RvE1 specifically inhibits TRPV1 signaling (*17*), whereas RvD1 attenuates the function of TRPA1 and TRPV4 (*18*) and RvD2 inhibits TRPV1 and TRPA1 activity (*19*). These effects have been observed with other types of n-3 PUFAs, such as maresin 1 (Mar1), which also has inhibitory effects on TRPV1 channel function (*20*) and reduces pain. The quantification of Rvs in the knee synovia of patients suffering from

inflammatory arthritis suggests that synthesis of specialized proresolving mediators (SPMs) at the site of inflammation may be a mechanism of endogenous pain relief in humans. In contrast, n-6 PUFA metabolites are pro-nociceptive by stimulating nerve fibers through the activation of immune cells (*21*, *22*). Nonetheless, several n-6 PUFA metabolites, such as thromboxane A_2 (TXA_2), PGE_2, leukotriene B_4 (LTB_4), and PGD_2, can directly stimulate sensory nerve fibers (*23*-*26*). However, some n-6 PUFA metabolites, such as lipoxins, can inhibit pain (*27*). Consistent with the role of TRP channels in the transduction of noxious stimuli, we previously showed a correlation between PUFA metabolites and TRP channel activation, particularly for the TRPV4 agonist 5,6-epoxyeicosatrienoic acid (5,6-EET) and pain intensity in IBS-D patients (*4*). Furthermore, PUFA metabolites from colonic biopsies of IBS-C patients induced Ca^{2+} influx in sensory neurons independently of TRPV4, suggesting that the PUFA metabolites produced in IBS-C and IBS-D are distinct (*4*). Thus, the aim of this study was to identify algogenic PUFA metabolites specifically produced in IBS-C patients and decipher the mechanism by which they may activate sensory nerves. Herein, we showed that 5-oxoETE, an n-6 PUFA subtype selectively increased in abundance in colonic tissues from IBS-C patients, induced hypersensitivity in a manner dependent on the G protein–coupled receptor (GPCR) Mrgprd.

Results

5-oxoETE is increased in abundance in colonic biopsies from IBS-C patients

PUFA metabolites were quantified in colonic biopsies from IBS patients and healthy controls (HCs) using liquid chromatography/tandem mass spectrometry (LC-MS/MS). Hierarchical clustering of PUFA metabolite amounts quantified in biopsies (pg/mg of protein) was used to reveal the main differences between HCs, IBS-M, IBS-C, and IBS-D patients (Fig. 1A). PUFA

metabolites formed five different clusters. The first cluster contained products of arachidonic acid metabolism (PGE_2, TXB_2, 5,6-EET, and 14,15-EET), eicosapentaenoic acid metabolism (18-HEPE, LtB5, and PGE_3) and protectin Dx (PDx). Metabolites belonging to this first cluster were most abundant in biopsies from IBS-D patients (Fig. 1A). Note that TxB_2, PGE_2, and 5,6-EET were only increased in biopsies of IBS-D patients (fig. S1). In contrast, TxB_2 was decreased in abundance in biopsies from IBS-C patients (fig. S1). The second cluster discriminated only 5-oxoETE, which was substantially increased in biopsies from IBS-C patients (Fig. 1, A and B). The concentrations of 7-MaR1 and $15dPGJ_2$, which delineated a third cluster, showed an increasing trend, but did not reach statistical significance in biopsies from any group of IBS patients (fig. S2). The fourth cluster, grouping most of the lipoxygenase-derived metabolites, was decreased in biopsies from all subtypes of IBS patients compared to HCs (Fig. 1A). 15-HETE, 5-HETE, 12-HETE, 14-HDoHE, and 17-HDoHE were statistically significantly decreased in abundance in all IBS patients (fig. S2). In addition, 12-HETE was statistically significantly decreased in abundance in biopsies from IBS-C patients (fig. S1). The metabolites included in the fifth cluster were reduced in amount only in biopsies from IBS-C and IBS-D patients (Fig. 1A). RvD1 and RvD2 were not detectable in any colonic biopsies. Thus, among all of the PUFA metabolites quantified in colonic biopsies from IBS patients, 5-oxoETE was the only one to be statistically significantly increased in IBS-C patients compared to the other IBS subtypes (Fig. 1B) and thus warranted further investigation.

Local administration of 5-oxoETE induces somatic and visceral hyperalgesia without inflammation

Because PUFA metabolites can stimulate the immune system, directly stimulate nerves, or both,

we first assessed the effect of 5-oxoETE on pain and inflammation processes *in vivo.* In a first set of experiments, 5-oxoETE was subcutaneously injected into the paws of mice and the paw-withdrawal threshold to mechanical stimuli was estimated using calibrated von Frey filaments. The time course of mechanical hypersensitivity of the mice that received 5-oxoETE was compared with that of mice injected with vehicle (HBSS). Basal mechanical sensitivity, measured in the paw before injection, was identical in both groups of mice (Fig. 2A). Injection of 5-oxoETE into the hind paws resulted in a decrease in the paw-withdrawal threshold (Fig. 2A) and was observed from 15 min up to 2 hours after 5-oxoETE injection, with maximal reduction at 30 min. The mechanical pain threshold was decreased in a dose-dependent manner 30 min after 5-oxoETE administration with an EC_{50} of 0.6 µM (Fig. 2B). In addition, paw edema formation and histological analysis were investigated to verify whether injection of 5-oxoETE induced an inflammatory process. Injection of 5-oxoETE into the hind paw did not induce paw edema (fig. S3). Moreover, histological analysis of paw tissue did not reveal any sign of inflammation. Similarly, neither tissue disruption nor cellular infiltration was observed even 6 hours after the injection of 100 µM 5-oxoETE (Fig. 2C). Thus, at the somatic level, 5-oxoETE increased paw sensitivity to mechanical stimulation without inducing a quantifiable inflammatory reaction.

Intracolonic administration of 5-oxoETE resulted in an increased intensity of abdominal contractions in response to colorectal distension (Fig. 2D). Moreover, the increased intensity of abdominal contractions was observed in response to both innocuous (15 mmHg; allodynia) and noxious (30 to 60 mmHg; hyperalgesia) stimuli 30 min after 5-oxoETE treatment (Fig. 2D). Intracolonic treatment with vehicle (40% ethanol) did not alter abdominal contraction response (Fig. 2D). As was observed after the subcutaneous injection of hind paws, intracolonic

administration of 5-oxoETE did not induce inflammation of the colon. Colonic inflammation was assessed by macroscopic scoring and myeloperoxidase activity, which were not increased by 5-oxoETE administration when compared to vehicle (fig. S3). Moreover, histological analysis did not reveal intestinal wall thickening, leukocyte infiltration into the *lamina propria,* the presence of ulceration, or goblet cell depletion (Fig. 2E). Thus, *in vivo* local administration of 5-oxoETE induced visceral hyperalgesia in the absence of inflammation, thus suggesting a direct effect on nociceptors.

5-oxoETE stimulates visceral and somatic nociceptors: translation to human DRG

To confirm a direct effect of 5-oxoETE on sensory nerve terminals innervating the colon, we examined its effects upon action potential firing in mouse colonic nociceptors. Specifically, we made teased-fiber electrophysiological recordings from the lumbar splanchnic nerve innervating the distal colon, which is primarily composed of colonic nociceptors with endings on serosal blood vessels penetrating the colon and in the mesentery. On defined populations of nociceptors with receptive fields isolated in flat sheet preparations, we applied 100 µM 5-oxoETE to a small chamber placed directly over the receptive field. 5-oxoETE stimulated action potential firing greater than vehicle in 38% of colonic nociceptor endings assessed (Fig. 3). In a second set of experiments, we determined the effect of 5-oxoETE on Ca^{2+} mobilization in primary cultures of neurons from mouse DRGs. In preliminary experiments performed with a working solution containing Ca^{2+} and Mg^{2+}, we observed a transient increase in the concentration of intracellular Ca^{2+} ($[Ca^{2+}]_i$) (fig. S4). To determine whether this transient increase was the consequence of intracellular Ca^{2+} release or influx of external Ca^{2+}, experiments were performed without Ca^{2+} and Mg^{2+} in the extracellular solution. Even without Ca^{2+} in the extracellular compartment, 5-oxoETE

evoked a transient increase in $[Ca^{2+}]_i$ that was maximal after 10 to 20 s and declined thereafter (Fig. 4A). The mobilization of intracellular Ca^{2+} by 5-oxoETE was concentration-dependent (Fig. 4B). Similarly, 5-oxoETE induced an increase in $[Ca^{2+}]_i$ and the percentage of responding neurons in a concentration-dependent manner in human primary sensory neurons (Fig. 4C). Thus, our data suggest that 5-oxoETE directly activates colonic DRG neurons from mice, as well as human sensory neurons, inducing an increase nociceptor firing (Fig. 3) and in $[Ca^{2+}]_i$ (Fig. 4).

Because 5-oxoETE induced somatic pain without inflammation *in vivo*, we hypothesised that 5-oxoETE predominantly activates $IB4^+$ sensory neurons, which do not release neuropeptides involved in neurogenic inflammation. To assess our hypothesis, we labelled mouse sensory neurons with isolectin B4 and treated the with 10 µM 5-oxoETE in the absence of extracellular Ca^{2+}. We found that 5-oxoETE induced an increase in $[Ca^{2+}]_i$ in >50% of the IB4-positive neurons, but not in IB4-negative neurons (Fig. 4D). To decipher the intracellular pathway responsible for the intracellular Ca^{2+} mobilization by 5-oxoETE, we pretreated mouse sensory neurons with pertussis toxin (PTX), which inhibits G_i family G proteins, or the PLC inhibitor U73122. In neurons pretreated with PTX (250 ng/ml), the increase in $[Ca^{2+}]_i$ induced by 5-oxoETE was statistically significantly decreased (Fig. 4E). Pre-treatment of sensory neurons with 10 µM U73122 also inhibited the increase in $[Ca^{2+}]_i$ induced by 5-oxoETE (Fig. 4E). Thus, these data suggest that 5-oxoETE directly stimulates IB4-positive sensory neurons through a $G\alpha_{i/o}$- and $G\alpha_q$-coupled GPCR.

5-oxoETE activates sensory neurons and induces visceral hypersensitivity through Mrgprd

Because we found that 5-oxoETE specifically activated $IB4^+$ sensory neurons through $G\alpha_i$-

mediated signalling pathways, we focused our attention on the MAS-related G protein receptor D (Mrgprd), which couples to $G\alpha_{i/o}$ and $G\alpha_q$ proteins. The expression and function of Mrgprd in polymodal nociceptors innervating the skin is well established (*28*); however, for visceral tissues, this remains less clear. To comprehensively assess this, we retrogradely labelled sensory afferents from the colon using microinjection of Fast Blue (FB) in wild-type mice and *Mrgprd*^{EGFP} mice. Single-cell qRT-PCR analysis was performed on FB-expressing cells from the DRGs of WT mice. We were able to detect *Mrgprd* mRNA at some level in 40% (18/45) of the FB-labelled sensory neurons projecting to the colon through the splanchnic nerve originating from the thoracolumbar (T10-L1) DRG (Fig. 5A). We detected *Trpv1* mRNA in 82% (37/45) of cells, with 41% (15/37) of the *Trpv1*-positive neurons also expressing *Mrgprd* mRNA (Fig. 5A). Immunohistochemistry was performed on the T13 DRG from the *Mrgprd*^{EGFP}-expressing mice to determine the incidence of GFP expression and the peptidergic marker calcitonin gene-related peptide (CGRP) in FB-labelled cells, which revealed two distinct non-overlapping populations (Fig. 5B). Consistent with previous studies, those sensory neurons labelled from the colon with the retrograde tracer Fast-Blue were predominantly CGRP-positive (~70%). In contrast, GFP immunoreactivity was observed in a restricted subset of colonic sensory neurons, accounting for only 7% of FB-labelled cells (Fig. 5B and Table 2). Of the 274 FB^+ cells assessed, only one cell co-expressed both Mrgprd and CGRP. Those neurons projecting to the viscera represented ~10% of the total population of T10-L1 DRG neurons. Thus, only a very small population (between less than 1% and 4%) of T10-L1 DRG neurons are likely to be both colon-projecting and Mrgprd-positive.

In experiments using an antibody against Mrgprd, we observed infrequent, yet reproducible, co-localisation of Mrgprd with PGP9.5 in the colon sections of 6 WT mice of 10 that were assessed

(fig. S5). Note that Mrgprd immunoreactivity was not observed in the colons of *Mrgprd*-deficient mice (fig. S6). The expression of Mrgprd in human sensory neurons was also assessed. We found that Mrgprd immunoreactivity was present in 22% of human T11 DRG neurons (Fig. 5C), which also co-expressed the pan-neuronal marker PGP9.5. In a culture of human sensory neurons, 20% of PGP9.5-positive neurons showed Mrgprd immunoreactivity (Fig. 5D).

To demonstrate the role of Mrgprd in 5-oxoETE–induced neuronal firing, we knocked it down by transducing primary cultures of mouse sensory DRG neurons with a recombinant lentivirus expressing a shRNA directed against *Mrgprd* and the gene reporter red fluorescent protein (RFP). As a control, neurons were transduced with a lentivirus expressing a scrambled shRNA. As expected, the percentage of neurons that responded to 5-oxoETE was statistically significantly reduced in sensory neurons expressing the *Mrgprd*-specific shRNA compared to those neurons expressing the scrambled shRNA (Fig. 6A). Accordingly, application of 5-oxoETE on sensory neurons from *Mrgprd*-deficient mice had no greater effect than the application of HBSS alone (Fig. 6B). In contrast, treatment of sensory neurons from *Mrgprd*-deficient mice with a mixture of GPCR agonists (bradykinin, serotonin, and histamine, each at 10 μM), which was used as a positive control, induced an increase in $[Ca^{2+}]_i$ (Fig. 6B). Reciprocally, 5-oxoETE induced a concentration-dependent increase in $[Ca^{2+}]_i$ only in transfected, *Mrgprd*-expressing CHO cells (Fig. 6C). Finally, we assessed the sensitivity of *Mrgprd*-deficient mice to colorectal distension 30 min after intracolonic administration of 10 μM 5-oxoETE. 5-oxoETE did not induce hypersensitivity in response to colorectal distension in *Mrgprd*-deficient mice (Fig. 6D).

Discussion

In this study, we showed that: (i) Concentrations of the PUFA metabolite 5-oxoETE were statistically significantly increased in biopsies from patients with IBS-C compared to biopsies from patients with other IBS subtypes or from HCs; (ii) 5-oxoETE induced somatic, as well as visceral, hyperalgesia, without promoting inflammation; (iii) 5-oxoETE activated both mouse and human sensory neurons; (iv) In mice, 5-oxoETE signaled in a manner dependent on Mrgprd. Together, these data suggest a role for 5-oxoETE and Mrgprd-expressing, IB4-positive sensory neurons in visceral hypersensitivity in IBS-C patients.

Eicosanoids and docosanoids are the most important lipids implicated in inflammatory processes. They derive from the oxidation of twenty and twenty-two carbon PUFAs, respectively (*29*). Several PUFA metabolites are increased in abundance in the intestinal mucosa from patients with IBDs (including, TXA_2, PGE_2, LTB_4, and PGD_2), which induce visceral afferent fiber activation (*23-26*). Here, we showed that PGE_2, 5,6-EET, and TXB_2 were statistically significantly increased in abundance in the intestinal mucosa of IBS-D patients, whereas no alteration in PUFA metabolism was observed in patients with IBS-M. Furthermore, when lipid extracts from HCs and all IBS patients were compared, we observed a statistically significant decrease in the amounts of 14-HDoHE and 17-HDoHE ,which are SPM precursors (*30*). Because SPMs possess an analgesic effect (*31*), the pain associated with IBS could be also the consequence of a decrease in SPM abundance, leading to sensory neuron activation. A complete characterization of the different SPMs produced by the metabolism of EPA, DHA, or DPA will be of interest for the characterization of bioactive lipids potentially linked with pain in IBS patients.

We showed that the concentration of 5-oxoETE increased in only the colonic biopsies of IBS-C patients, highlighting its potential relevance as a new marker of this disease. 5-oxoETE, which derives from arachidonic acid (AA) metabolism, is produced by various inflammatory cells. In addition, it can also be synthesized from 5-HETE by stromal cells, possibly by transcellular biosynthesis (*32*). 5-oxoETE is formed by the oxidation of 5-HETE by 5-hydroxyeicosanoid dehydrogenase (5-HEDH) (*33*), a microsomal enzyme that is highly selective for 5S-HETE and requires $NADP^+$ as a cofactor (*34*). 5-HEDH is found in neutrophils as well as in various other inflammatory and stromal cells, including monocytes (*35*), dendritic cells (*36*), and intestinal epithelial cells (*37*). 5-oxoETE is a potent chemoattractant for human and rat eosinophils and it indirectly promotes the survival of these cells (*38*). However, we observed no cellular infiltration either in the paw or intestinal mucosa of mice administered with 5-oxoETE. This discrepancy may be due to the rapid metabolism of 5-oxoETE *in vivo* (*32*) or the absence of other molecules, such as interleukin-5, which act in synergy to attract inflammatory cells during inflammatory processes or allergies (*39*). In our experiments, the injection of 5-oxoETE alone, without cofactors, could thus explain the absence of infiltration of tissues by polymorphonuclear cells. The formation of 5-oxoETE requires $NADP^+$ (*40*). Accordingly, oxidative stress associated with IBS-C (*41*) may improve the conversion rate of NADPH into $NADP^+$ in epithelial cells, thereby resulting in the synthesis of greater amounts of 5-oxoETE.

In a previous study, we reported that PUFA metabolites extracted from biopsies of IBS-C and IBS-D patients triggered an increase in $[Ca^{2+}]_i$ in primary sensory neurons, whereas those extracted from biopsies of IBS-M patients had no effect (*4*). We further identified the PUFA metabolite 5,6-EET as a TRPV4 agonist with algogenic activity, specifically associated with IBS-D sub-group

(*4*). By contrast, no PUFA metabolite with TRP agonist activity was found to be increased in abundance in IBS-C patient biopsies (*4*). Because we found that only 5-oxoETE was increased in biopsies of IBS-C patients, we hypothesized that this PUFA metabolite might be responsible for the activation of sensory neurons and hypersensitivity-associated with IBS-C. As previously reported in humans, 5-oxoETE may interact with the oxoeicosanoid receptor 1 (OXER1). However, there is no homologous OXE receptor in rodents (*40*). Because the observed 5-oxoETE-–nduced increase in $[Ca^{2+}]_i$ in mouse sensory neurons was inhibited by both a PLC inhibitor and PTX, we hypothesized that 5-oxoETE led to the activation of $G\alpha_{i/o}/G\alpha_q$-coupled GPCRs. Given that 5-oxoETE acted selectively on $IB4^+$ sensory neurons, the targeted receptor should be specifically expressed on this neuronal subclass. Accordingly, we investigated the role of Mrgprd, a GPCR specifically expressed on $IB4^+$ sensory neurons, which may be coupled to $G\alpha_q$ proteins and to PTX–sensitive $G\alpha_{i/o}$ proteins (*42*), and was previously reported as a key player in mechanical hypersensitivity (*43-45*).

Stimulation of Mrgprd-positive neurons with β-alanine, the prototypical agonist of Mrgprd, increases $[Ca^{2+}]_i$ (*46*), as was observed here after 5-oxoETE treatment. Moreover, in a FLIPR (Fluorescent Imaging Plate Reader) assay developed for the simultaneous identification of Mrgprd agonists and antagonists, a PLC inhibitor completely blocked the FLIPR response to β-alanine, whereas PTX treatment resulted in 50% reduction in $[Ca^{2+}]_i$ (*47*). Again, similar results were obtained here in experiments with PTX or a PLC inhibitor to inhibit 5-oxoETE–induced activation of primary mouse sensory neurons. Using tissue from adult $Mrgprd^{EGFP}$ mice stained with antibodies to GFP, a previous study showed that Mrgprd is expressed in non-peptidergic neurons that innervate the epidermis; however, Mrgprd-positive fibres were not observed in any other

visceral organs, including both the small and large intestine (*28*). By contrast, numerous studies using different retrograde tracers have identified a minor population (20 to 26%) of $IB4^+$ sensory neurons that innervate the colon (*48-50*). Indeed, a study also identified *Mrgprd* mRNA in colonic sensory neurons by single cell RNA-sequencing (*51*). To confirm the presence of both *Mrgprd* mRNA and Mrgprd protein in colonic sensory neurons in the present study, we applied a similar retrograde neurotracing approach using single-cell RT-qPCR analysis and anti-GFP immunostaining in $Mrgprd^{EGFP}$ mice. We observed *Mrgprd* mRNA and Mrgprd protein expression in sensory DRG neurons projecting to the colon at a similar frequency to that observed in previous studies (*51*), thereby not only confirming the presence of a Mrgprd-positive colonic neuronal subtype, but also reinforcing Mrgprd as a potential target of 5-oxoETE. The activity of 5-oxoETE towards Mrgprd was attested to by its ability to induce an increase in $[Ca^{2+}]_i$ in IB4-positive sensory neurons, but not in mouse neurons in which *Mrgprd* was knocked down by shRNA or in neurons from *Mrgprd*-deficient mice. Conversely, whereas Ca^{2+} transients were stimulated by 5-oxoETE in CHO cells transfected with a plasmid expressing *Mrgprd*, CHO cells transfected with a control plasmid were not responsive to 5-oxoETE.

Activation of Mrgprd inhibits a fraction of the total M-current, carried primarily by the KCNQ2/3 K^+ channel, contributing to an increase in the excitability of DRG neurons (*52*). Thus, Mrgprd activation by 5-oxoETE might promote the excitability of primary nociceptive afferents by KCNQ inhibition. Several groups have demonstrated that retigabine, a KCNQ2–5 opener, is effective in reducing neuropathic (*53*) and inflammatory pain (*54*). At the visceral level, retigabine reduces capsaicin-induced visceral pain and can inhibit noxious chemosensitivity in human tissue, suggesting that KCNQ channels play an inhibitory role in the transmission of visceral nociception

(*55, 56*). Given that human sensory DRG neurons express Mrgprd and are activated by 5-oxoETE, we can speculate that 5-oxoETE modulates KCNQ channels through Mrgprd activation, leading to neuronal activation that contributes to the pain symptoms associated with IBS-C. Nevertheless, because OXER1 is expressed in human tissue, we cannot exclude the possibility that this receptor is activated by 5-oxoETE in human tissue. Together, our current findings build on our previous studies to suggest a pivotal role for PUFA metabolites in the visceral pain associated with IBS (*4*). Specifically, our study identifies 5-oxoETE with pro-nociceptive activity, as a hallmark of the IBS-C subtype.

Materials and methods

Chemicals

6-keto-prostaglandin F1α (6kPGF$_{1\alpha}$), thromboxane B$_2$ (TXB$_2$), prostaglandin E$_2$ (PGE$_2$), prostaglandin A$_1$ (PGA$_1$), 8-iso prostaglandin A$_2$ (8-iso PGA$_2$), prostaglandin E$_3$ (PGE$_3$), 15-deoxy-$\Delta^{12,14}$-prostaglandin J$_2$ (15d-PGJ$_2$), lipoxin A$_4$ (LxA$_4$), lipoxin B$_4$ (LxB$_4$), lipoxin A4 deuterated (LxA4-d5), resolvin D1 (RvD1), resolvin D2 (RvD2), 7-maresin (7-MaR1), leukotriene B$_4$ (LTB$_4$), leukotriene B$_5$ (LTB$_5$), leukotriene B$_4$ deuterated (LTB$_4$-d4), 10(S),17(S)-protectin (PDx), 18-hydroxyeicosapentaenoic acid (18-HEPE), dihydroxy-eicosatetraenoic acid (5,6-DiHETE), 15-hydroxyeicosatetraenoic acid (15-HETE) and 12-HETE, 8-HETE, 5-HETE, 5-HETE-d8, 17-hydroxy-docosahexaenoic acid (17-HDoHE) and 14-HDoHE, 14,15-epoxyeicosatrienoic acid (14,15-EET) and 11,12-EET, 8,9-EET, 5,6- EET, 5-oxoeicosatetraenoic acid (5-oxoETE) were purchased from Cayman Chemicals.

Patients

Patients (Table 1) were recruited from outpatient clinics of the Department of Medical and Surgical Sciences of the University of Bologna (Italy), and were included according to the Rome III criteria for IBS. Healthy controls (HCs) were asymptomatic subjects undergoing colonoscopy for colorectal cancer screening. In this group, we excluded subjects based on the presence of the following symptoms in the previous 12 months: abdominal discomfort or pain, bloating, and bowel habit changes. Exclusion criteria for both IBS and HC included major abdominal surgery, any organic syndrome, celiac disease (excluded by detection of anti-transglutaminase and anti-endomysial antibodies), asthma, food allergy, or other allergic disorders. None of these patients or HCs were taking nonsteroidal anti-inflammatory drugs or any other anti-inflammatory drugs (including steroids, antihistamines, and mast cell stabilizers). Patients and HCs gave written informed consent. The study protocol was approved by the local Ethic Committee (64/2004/O/Sper and EM14/2006/O) and conducted in accordance with the Declaration of Helsinki. Patients underwent colonoscopy, and, in all cases, 6 mucosal biopsies were obtained from the proximal descending colon. One biopsy was sent to the pathology department for exclusion of microscopic colitis or other microscopic tissue abnormalities and 4 were used in other studies. One biopsy was snap-frozen in liquid nitrogen for lipid extraction and PUFA quantification for the purpose of our study.

Lipid extraction

Biopsies were crushed with a FastPrep-24 Instrument (MP Biomedicals) in 500 µL of Hanks' balanced salt solution (HBSS, Invitrogen) and 5 µL of internal standard mixture (LxA4-d5, LTB4-d4, and 5-HETE-d8 at 400 ng/mL in MeOH). After 2 crush cycles (6.5 m/s, 30 s), 10 µL were withdrawn for protein quantification and 300 µL of cold methanol were added. Samples were

centrifuged at 1000 g for 15 min at 4 °C. Supernatants were collected, adjusted to 2 mL in H_2O, and submitted to solid-phase extraction using HRX-50 mg 96-well (Macherey Nagel). Briefly, after plate conditioning, the sample was loaded at flow rate of 0.1 mL/min. After complete loading, the plate was washed with H_2O/MeOH (90:10, 2 mL) and lipid mediators were eluted with MeOH (2 mL). Solvent was evaporated under nitrogen and samples were dissolved with MeOH and stored at -80 °C for liquid chromatography/tandem mass spectrometry measurements.

Liquid chromatography/tandem mass spectrometry (LC-MS/MS) measurements

6kPGF1α, TXB_2, PGE_2, PGA_1, 8-isoPGA_2, PGE_3, 15d-PGJ_2, LxA4, LxB4, RvD1, RvD2, 7-MaR1, LTB4, LTB5, PDx, 18-HEPE, 5,6-DiHETE, 15-HETE, 12-HETE, 8-HETE, 5-HETE, 17-HDoHE, 14-HDoHE, 14,15-EET, 11,12-EET, 8,9-EET, 5,6-EET and 5-oxo-ETE were quantified in human biopsies (*57*). To simultaneously separate 28 lipids of interest and 3 deuterated internal standards, LC-MS/MS analysis was performed on an ultra high-performance liquid chromatography system (UHPLC, Agilent LC1290 Infinity) coupled to an Agilent 6460 triple quadrupole MS (Agilent Technologies) equipped with electro-spray ionization operating in negative mode. Reverse-phase UHPLC was performed using a ZorBAX SB-C18 column (Agilent Technologies) with a gradient elution. The mobile phases consisted of water, acetonitrile (ACN), and formic acid (FA) (75:25:0.1; v/v/v) (Solution A) and ACN, FA (100:0.1, v/v) (Solution B). The linear gradient was as follows: 0% Solution B at 0 min, 85% Solution B at 8.5 min, 100% Solution B at 9.5 min, 100% Solution B at 10.5 min and 0% Soution B at 12 min. The flow rate was 0.35 mL/min. The autosampler was set at 5°C and the injection volume was 5 µL. Data were acquired in Multiple Reaction Monitoring (MRM) mode with optimized conditions. Peak detection, integration, and quantitative analysis were performed with Mass Hunter Quantitative

analysis software (Agilent Technologies). For each standard, calibration curves were built using 10 solutions at concentrations ranging from 0.95 to 500 ng/mL. A linear regression with a weight factor of 1/X was applied for each compound. The limit of detection (LOD) and the limit of quantification (LOQ) were determined for the 28 compounds using signal to noise (S/N) ratios. The LOD corresponded to the lowest concentration leading to a S/N value > 3 and LOQ corresponded to the lowest concentration leading to a S/N value > 10. All values less than the LOQ were not considered. Blank samples were evaluated, and their injection showed no interference (no peak detected), during the analysis. Hierarchical clustering was performed and heat-maps were obtained with R (www.r-project.org). PUFA metabolite amounts were transformed to z-scores and clustered based on 1-Pearson correlation coefficient as distance and the Ward algorithm as agglomeration criterion.

Animals

C57BL/6 male mice (3 weeks-old) were purchased from Janvier. *Mrgprd*$^{cre/+}$ mice were a generous gift from D. Anderson (Caltech, Pasadena). These mice were previously generated as described by Rau *et al*. (*44*) and were in an almost pure C57/Bl6J background when we received them at the IBDM (Institut de Biologie du Développement de Marseille) mouse facility. There, the mice were kept as heterozygotes and were backcrossed to C57/Bl6J for another 8 generations. *Mrgprd*-deficient mice used in this study were obtained by intercrossing *Mrgprd*$^{cre/+}$ heterozygous mice. Animals were maintained in ventilated cages (4 mice per cage) in a specific pathogen–free room at 20 to 24°C and relative humidity (40 to 70%) with a 12-hour light/dark cycle and given free access to food and water. Animal Care and ethic Committee of US006/CREFE (CEEA-122) approved the whole study protocol (permit No. MP/01/64/09/12). *Mrgprd*^{EGFP} mice (B6;129SP2-

Mrgprd$^{tm4.1(COP4)Mjz}$/Mmnc; MMRRC, North Carolina, USA) were raised and maintained at the University of Glasgow and were characterized previously (*58*). Experiments conducted at the University of Glasgow were approved by the University's Ethical Review Process Applications Panel and were performed in accordance with the European Community directive 86/609/EC and the United Kingdom Animals (Scientific Procedures) Act 1986.

Measurement of somatic nociception

Paw-withdrawal thresholds were measured using calibrated von Frey filaments with forces ranging from 0.04 to 2 g (Stoelting), which were applied onto the plantar surface of the mice. An ascending series of von Frey filaments was applied with each monofilament being tested 5 times for approximately 1 s. Threshold to mechanical stimuli was calculated as the force value of the von Frey filament triggering 3 paw withdrawals over 5 applications (*59*). Responses to mechanical stimuli were recorded before and 15 min, 30 min, 1 hour, 2 hours, and 6 hours after an intraplantar injection of 0.1, 1, 10, or 100 μM 5-oxoETE or vehicle (HBSS). In a second set of experiments, paw edema was measured using a digital caliper (resolution 0.01; Mitutoyo, Aurora, IL, USA) at 1, 2, 3 and 4 hours after intraplantar injection of 100 μM 5-oxoETE. At the end of the experiment, paws were collected for histological analysis by hematoxylin and eosin (H&E) staining.

Colorectal distension (CRD) and electromyography recordings

Mice were administered either 100 μL of 5-oxoETE (10 μM) or vehicle (40% ethanol) intracolonically. We performed a session of CRD and recorded visceromotor responses (VMRs) from implanted electrodes before and 30 min after treatment as previously described (*60*). Data are presented as the difference between the VMR induced by the distension performed before and

after intracolonic treatments. After distension, mouse colons were harvested to perform histological (H&E) analysis and myeloperoxidase activity assay.

Lumbar splanchnic nerve recording

The distal colon with associated lumbar splanchnic nerves was removed from male C57BL/6 mice (12 weeks old). The colon was then opened along the anti-mesenteric border and pinned flat, mucosal side up. The tissue was perfused (7 mL/min; 32 to 34℃) with carbogenated Krebs buffer (124 mM NaCl, 4.8 mM KCl, 1.3 mM NaH_2PO_4, 2.4 mM $CaCl_2$, 1.2 mM $MgSO_4.7H_2O$, 11.1 mM glucose, 25 mM $NaHCO_3$) and supplemented with 10 µM nifedipine and 10 µM atropine to block smooth muscle contraction, and 3 µM indomethacin to inhibit endogenous prostanoid production. Single unit activity was discriminated using wave form analysis software (Spike 2 Cambridge Electronic Design) from fibers teased from the lumbar splanchnic nerve (rostral to the inferior mesenteric ganglia), recorded using borosilicate glass suction electrodes. Signals were amplified, band pass filtered (gain 5K; 100-1300 Hz; Neurology, Digitiser Ltd, UK), digitally filtered for 50Hz noise (Humbug, Quest Scientific, Canada), digitalised at 20 kHz (micro1401; Cambridge Electronic Design, UK), and displayed on a computer using Spike 2 software. Individual receptive fields of afferent nerve fibers were identified by systematically probing the tissue with a 1-g von Frey filament. Receptive fields that responded to probing and not to stretch were identified as serosal units (*61*). Once a serosal unit was identified, a metal ring was placed over the receptive field and the baseline activity was observed for 3 min. The Krebs solution within the ring was then removed and replaced by 100 µM 5-oxoETE pre-warmed to bath temperature. Following a 7-min challenge period, the 5-oxoETE and ring were removed.

Immunofluorescence in mouse colon

The descending colons of 10 WT and 10 *Mrgprd*-deficient mice were cryoprotected in OCT compound, sectioned at a thickness of 10 µm (one every 0.1 cm, 20 per mouse) on a cryostat (Leica CM1950, Nanterre, France), and mounted on Superfrost slides (Thermo Fisher Scientific, Villebonne-sur-Yvette, France). Slides were washed in phosphate-buffered saline (PBS), 0.5% Triton X-100, and 1% bovine serum albumin (BSA) solution (Sigma), and incubated overnight at 4°C with anti-Mrgprd (1:500, AMR-061, Alomone labs, Clinisciences, Nanterre, France) and anti-PGP9.5 (1:500, AB86808, Abcam, Coger SAS, Paris, France) as primary antibodies. After washing, slides were incubated with the appropriate secondary antibody conjugated with Alexa Fluor 488 or Alexa Fluor 555 (Thermo Fisher Scientific), washed, and mounted with ProLong Gold reagent containing DAPI (Molecular Probes). Images were acquired using a Zeiss LSM-710 confocal microscopes (Carl Zeiss MicroImaging, Jena, Germany) with 20X objective in the inverted configuration.

Single-cell qRT-PCR analysis of retrogradely labelled mouse sensory neurons

DRG neurons projecting to the colon were selectively labelled and individually harvested by pulled glass pipette. After RNA extraction, single-cell RT-qPCR analysis for the presence of *Mrgprd* mRNA transcripts was performed as previously described (*62*). Briefly, adult mice were subjected to laparotomy under anesthesia and 6 to 8 injections of Fast Blue (~ 0.2 µL, 2 % in saline; Polysciences GmbH) were made into the wall of the distal colon. Five days after surgery, thoracolumbar (TL; T10-L1) DRGs were collected and enzymatically dissociated (*62*). Individual cells were isolated by pulled glass pipette and collected into a preamplification mastermix containing 0.1 µL SUPERase-in (Ambion, TX, USA), 0.2 µL Superscript III Reverse

Transcriptase/Platinum Taq mix (Invitrogen), 5 μL CellDirect 2x reaction buffer (Invitrogen), 2.5 μL 0.2x primer/probe mix, and 1.2 μL TE buffer (Applichem, GmbH) before thermal cycling [50°C for 30 min, 95°C for 2 min, and then 21 cycles of (95°C for 15 s, 60°C for 4 min)]. TaqMan qPCR assays for *Mrgprd* (TaqMan Assay ID: Mm01701850_s1) and *Trpv1* (Mm01246300_m1) were performed on diluted cDNA products (1:5 in TE buffer) using the following cycling protocol: 50°C for 2 minutes, 95°C for 10 minutes, then 40 cycles of (95°C for 15 seconds, 60°C for 1 minutes). *Glyceraldehyde-3-phosphate dehydrogenase* (*Gapdh*) mRNA acted as an internal positive control and a sample of the bath solution was used as a no-template negative control. Sll single-cell RT-PCR products contained *Gapdh* mRNA, whereas bath control samples did not. The quantitative assessment of gene expression was determined by quantification of cycle (Cq) values less than the threshold of 35 that were considered as positive. In total, 15 single cells per spinal region (TL) per mouse (n = 3 mice) were isolated; therefore, the expression of mRNA transcripts was determined in 45 colonic sensory neurons.

Immunohistochemistry of Fast Blue–labelled colonic sensory neurons from *Mrgprd*^{EGFP} mice

From thoracolumbar regions, DRG T13 were stained from four *Mrgprd*^{EGFP} mice retrogradely labelled with Fast Blue to the colon, as described earlier. A single T13 DRG was sectioned sequentially across 10 slides at 12-μm thickness. Therefore, on a given slide, the T13 DRG was sampled at 120-μm intervals for the full thickness of the DRG. In total, 16 sections from 4 animals were analysed, yielding 274 Fast Blue–labelled cells. Slides were stained with chicken anti-GFP (1:1000; Abcam Ab13790) and rabbit anti-CGRP (1:10000, Sigma C8198) antisera. The secondary antibodies used were goat anti-chicken-488 (1:1000) and donkey anti-rabbit-594 (1:1000). Each probe (that is, *Mrgprd*^{EGFP} and CGRP) per section had a background reading subtracted and was

normalized between the maximum and minimum intensity cells. A threshold of mean + 3× SD for the minimum intensity cells (from all 16 sections) was used to differentiate positive from negative cells. Positive cells were then manually confirmed.

Ca^{2+} imaging of mouse sensory neurons

DRGs of WT and *Mrgprd*-deficient mice were rinsed in cold HBSS (Invitrogen), and enzymatically dissociated as described previously (*63*). Neurons were plated in 96-well plates (fluorescence Greiner bio one, Domique Dutscher, Brumath, France) and cultured for 24 hours. In a first set of experiments, neurons were treated with 5-oxoETE (1, 5, 25, 50, and 100 µM) or vehicle (HBSS). In a second set of experiments, neurons were incubated for 1 hour with 10 µg/mL isolectin B4 from Griffonia simplicifolia conjugated to Alexa Fluor 594 (ThermoFisher) to differentiate IB4-positive from IB4-negative sensory neurons. Ca^{2+} flux was monitored by recording the changing emission intensity of Fluo-4 (Molecular probe) after treatment with 5-oxoETE (10 µM) or vehicle. In a third set of experiments, neurons were pre-incubated with PTX (250 ng/mL) overnight or with the U73122 phospholipase C inhibitor (10 µM) 30 min before treatment with 5-oxoETE (50 µM) or vehicle.

Expression of shRNA directed against *Mrgprd* in sensory neurons

Lentiviral particles were produced as previously described (*64*). Briefly, HEK293T/17 cells (ATCC) were cultured according to the supplier's recommendations. Cells ($1.7x10^7$) were seeded into a 175-cm^2 culture flask containing 30 mL of DMEM (Gibco, USA) and then incubated at 37°C 5% CO_2. On the next day, cells were transfected with a mixture of structural (psPAX2 and pMD2.G; Addgene, Cambridge, MA, USA) and transfer vectors (shRNA Mrgprd-RFP-CB or the

control shRNA-RFP-CB; OriGene Technologies), with GeneJuice (Millipore, USA) transfection reagent. Cells were incubated overnight at 37°C and 5% CO_2 before the medium was replaced with 18 mL of OptiMEM (Gibco, USA). Cell culture medium were harvested 48 hours later and cleared by centrifugation and filtration with a 0.45-μm syringe filter. Neurons were plated in 96-well plates coated with poly-L-ornithine/laminin and cultivated in Neurobasal medium supplemented with B27 and L-glutamine before being transduced with 50 μL of lentiviral supernatant. Three days later, a transduction efficiency of 35% was achieved and a calcium flux assay was performed in response to 5-oxoETE (10 μM), as described earlier.

Ca^{2+} flux in CHO cells expressing Mrgprd

CHO cells were transfected with a plasmid expressing mouse *Mrgprd* (OriGene Technologies, Rockville, USA) with GeneJuice Transfection Reagent (1 μg of plasmid for 3 μL of GeneJuice). The cells were incubated in Ham's F12 Nutrient Mixture with 5% of FBS. G418 (Sigma) was used as the selection antibiotic. Cells (50×10^3 cells/well) in a 96-well plate were incubated with fluo-8 loading solution (Fluo-8-AM; Invitrogen) according to the manufacturer's instructions. The fluorescence was then measured at 530 nm on a microplate reader (NOVOstar; BMG Labtech) for 1 min. Five seconds after the beginning of the calcium measures, 5-oxoETE (1, 10, 25, 50, 100 and 200 μM) or β-alanine (Sigma-Aldrich; 1 mM) was added. Data were collected and analyzed with the NOVOstar software.

Ca^{2+} imaging of human sensory neurons

Experiments were conducted according to opinion number 14-164 of the institutional review board (IRB00003888) of the French institute of medical research and health. Three human T11 (thoracic

position 11) DRGs were supplied through the national human tissue resource center from the national disease resource interchange (NDRI). The DRGs were received unfixed in DMEM at 4°C. DRGs were dissected, minced in HBSS, and incubated in Papain (27 µg/mL) (Sigma, Saint Quentin Fallavier, France) for 20 min at 37°C. After a wash with L-15 Wash Buffer [Leibovitz's L-15 Medium (Invitrogen), 10% FBS (Invitrogen)] and HBSS, the DRGs were incubated in HBSS containing 1 mg/mL of collagenase type IV (Worthington, Lakewood, NJ, USA) and 4 mg/mL of dispase II (Sigma). L-15 Wash buffer was added to neutralize enzymatic activities and the suspension was centrifuged at 1000 g for 5 min. The cycle of digestion was repeated 3 times for 15 min. Neurons in the pellet were suspended in Neurobasal medium (Invitrogen) containing 2% B27, 2 mmol/L glutamine, 1% penicillin/streptomycin, and 10 µM each of cytosine arabinoside, 5-Fluoro-2′-deoxyuridine (FUDR), and Uridine (all from Sigma). The medium was changed every 3 days without cytosine arabinoside. Cells were plated in CC2 LabTek II (Nunc, Domique Dutscher, Brumath, France) for the calcium signalling assay as described earlier in response to 5-oxoETE (0.1, 1 and 10 µM) and for immunochemistry.

Immunofluorescence in human dorsal root ganglia

Experiments were performed according to opinion number 12-074 of the institutional review board (IRB00003888) of the French institute of medical research and health. Two human T11 (thoracic position 11) DRGs were supplied through the national human tissue resource center from the national disease resource interchange (NDRI). The DRGs were received unfixed and cryoprotected. The DRGs were cut into 20-µm sections on a cryostat (Leica CM1950, Nanterre, France), and mounted on Superfrost slides (Thermo Fisher Scientific, Villebonne-sur-Yvette, France). Cultured sensory neurons and slides were washed in PBS, 0.5% Triton X-100, and 1%

BSA solution (Sigma, Saint-Quentin Fallavier, France) and incubated overnight at 4°C with anti-Mrgprd (1:100, LS-A4123, LifeSpan Biosciences, Clinisciences, Nanterre, France) and anti-PGP9.5 (1:500, AB86808, Abcam). After washing, the slides and cultured DRG were incubated with the appropriate secondary antibody conjugated with Alexa Fluor 488 or Alexa Fluor 555, washed, and mounted with ProLong Gold reagent containing DAPI (Molecular Probes). Images were acquired using a Zeiss LSM-710 confocal microscope (Carl Zeiss MicroImaging, Jena, Germany) with a 20X objective in the inverted configuration.

Study approval

The study protocol for biopsy collection was approved by the local Ethic Committee (64/2004/O/Sper and EM14/2006/O) and conducted in accordance with the Declaration of Helsinki. Patients and HCs gave written informed consent. Fixed and fresh human DRGs were supplied through the national human tissue resource center from the national disease resource interchange (NDRI, reference: DCEN1 001). Experiments on human DRGs were performed according to opinion number 14-164 of the institutional review board (IRB00003888) of the French institute of medical research and health. Animal experiments were conducted according to the European union council directive 2010/63/EU. The Animal Care and ethic Committee of US006/CREFE (CEEA-122) approved the whole study protocol (permit No. MP/01/64/09/12). Experiments conducted at the University of Glasgow were approved by the University's Ethical Review Process Applications Panel and were performed in accordance with European Community directive 86/609/EC and the United Kingdom Animals (Scientific Procedures) Act 1986.

Statistical analysis

Data are presented as means ± standard error of the mean (SEM). Analyses were performed using GraphPad Prism 5.0 software (GraphPad, San Diego, CA). Comparisons between groups were performed by Mann-Whitney test. Multiple comparisons within groups were performed by Kruskal-Wallis test, followed by Dunn's post-test. Statistical significance was accepted at $P < 0.05$.

Supplementary Materials

Fig. S1. Concentrations of PUFA metabolites in biopsies from patients with IBS.
Fig. S2. Concentrations of PUFA metabolites in biopsies of all IBS patients.
Fig. S3. 5-oxoETE does not induce somatic or visceral inflammation in vivo.
Fig. S4. 5-oxoETE induces Ca^{2+} flux in mouse sensory neurons.
Fig. S5. Mrgprd immunoreactivity is observed in mouse colon.
Fig. S6. Mrgprd immunoreactivity is not observed in the colon of *Mrgprd*-deficient mice.

References and Notes

1. F. Mearin, B. E. Lacy, L. Chang, W. D. Chey, A. J. Lembo, M. Simren, R. Spiller, Bowel Disorders. *Gastroenterology*, (2016).
2. P. Enck, Q. Aziz, G. Barbara, A. D. Farmer, S. Fukudo, E. A. Mayer, B. Niesler, E. M. Quigley, M. Rajilic-Stojanovic, M. Schemann, J. Schwille-Kiuntke, M. Simren, S. Zipfel, R. C. Spiller, Irritable bowel syndrome. *Nat Rev Dis Primers* **2**, 16014 (2016).
3. L. Ohman, M. Simren, Pathogenesis of IBS: role of inflammation, immunity and neuroimmune interactions. *Nat Rev Gastroenterol Hepatol* **7**, 163-173 (2010).
4. N. Cenac, T. Bautzova, P. Le Faouder, N. A. Veldhuis, D. P. Poole, C. Rolland, J. Bertrand, W. Liedtke, M. Dubourdeau, J. Bertrand-Michel, L. Zecchi, V. Stanghellini, N. W. Bunnett, G. Barbara, N. Vergnolle, Quantification and Potential Functions of Endogenous Agonists of Transient Receptor Potential Channels in Patients With Irritable Bowel Syndrome. *Gastroenterology* **149**, 433-444 e437 (2015).
5. G. Barbara, B. Wang, V. Stanghellini, G. R. De, C. Cremon, N. G. Di, M. Trevisani, B. Campi, P. Geppetti, M. Tonini, N. W. Bunnett, D. Grundy, R. Corinaldesi, Mast cell-dependent excitation of visceral-nociceptive sensory neurons in irritable bowel syndrome. *Gastroenterology* **132**, 26-37 (2007).
6. G. Clarke, S. M. O'Mahony, A. A. Hennessy, P. Ross, C. Stanton, J. F. Cryan, T. G. Dinan, Chain reactions: Early-life stress alters the metabolic profile of plasma polyunsaturated fatty acids in adulthood. *Behavioural Brain Research* **205**, 319-321 (2009).
7. G. Clarke, P. Fitzgerald, A. A. Hennessy, E. M. Cassidy, E. M. Quigley, P. Ross, C. Stanton, J. F. Cryan, T. G. Dinan, Marked elevations in pro-inflammatory polyunsaturated fatty acid metabolites in females with irritable bowel syndrome. *J.Lipid Res.* **51**, 1186-1192 (2010).
8. S. Tokuyama, K. Nakamoto, Unsaturated fatty acids and pain. *Biol Pharm Bull* **34**, 1174-1178 (2011).

9. A. A. Berbert, C. R. Kondo, C. L. Almendra, T. Matsuo, I. Dichi, Supplementation of fish oil and olive oil in patients with rheumatoid arthritis. *Nutrition* **21**, 131-136 (2005).
10. P. C. Calder, Session 3: Joint Nutrition Society and Irish Nutrition and Dietetic Institute Symposium on 'Nutrition and autoimmune disease' PUFA, inflammatory processes and rheumatoid arthritis. *Proc Nutr Soc* **67**, 409-418 (2008).
11. Z. Harel, F. M. Biro, R. K. Kottenhahn, S. L. Rosenthal, Supplementation with omega-3 polyunsaturated fatty acids in the management of dysmenorrhea in adolescents. *Am J Obstet Gynecol* **174**, 1335-1338 (1996).
12. A. Belluzzi, S. Boschi, C. Brignola, A. Munarini, G. Cariani, F. Miglio, Polyunsaturated fatty acids and inflammatory bowel disease. *Am J Clin Nutr* **71**, 339S-342S (2000).
13. D. Miyazawa, A. Ikemoto, Y. Fujii, H. Okuyama, Dietary alpha-linolenic acid suppresses the formation of lysophosphatidic acid, a lipid mediator, in rat platelets compared with linoleic acid. *Life Sci* **73**, 2083-2090 (2003).
14. C. Ramsden, C. Gagnon, J. Graciosa, K. Faurot, R. David, J. A. Bralley, R. N. Harden, Do omega-6 and trans fatty acids play a role in complex regional pain syndrome? A pilot study. *Pain Med* **11**, 1115-1125 (2010).
15. A. M. Patwardhan, P. E. Scotland, A. N. Akopian, K. M. Hargreaves, Activation of TRPV1 in the spinal cord by oxidized linoleic acid metabolites contributes to inflammatory hyperalgesia. *Proc Natl Acad Sci U S A* **106**, 18820-18824 (2009).
16. J. Y. Lim, C. K. Park, S. W. Hwang, Biological Roles of Resolvins and Related Substances in the Resolution of Pain. *Biomed Res Int* **2015**, 830930 (2015).
17. Z. Z. Xu, L. Zhang, T. Liu, J. Y. Park, T. Berta, R. Yang, C. N. Serhan, R. R. Ji, Resolvins RvE1 and RvD1 attenuate inflammatory pain via central and peripheral actions. *Nat Med* **16**, 592-597, 591p following 597 (2010).
18. S. Bang, S. Yoo, T. J. Yang, H. Cho, Y. G. Kim, S. W. Hwang, Resolvin D1 attenuates activation of sensory transient receptor potential channels leading to multiple anti-nociception. *Br J Pharmacol* **161**, 707-720 (2010).
19. C. K. Park, Z. Z. Xu, T. Liu, N. Lu, C. N. Serhan, R. R. Ji, Resolvin D2 is a potent endogenous inhibitor for transient receptor potential subtype V1/A1, inflammatory pain, and spinal cord synaptic plasticity in mice: distinct roles of resolvin D1, D2, and E1. *J Neurosci* **31**, 18433-18438 (2011).
20. C. K. Park, Maresin 1 Inhibits TRPV1 in Temporomandibular Joint-Related Trigeminal Nociceptive Neurons and TMJ Inflammation-Induced Synaptic Plasticity in the Trigeminal Nucleus. *Mediators Inflamm* **2015**, 275126 (2015).
21. H. Harizi, J. B. Corcuff, N. Gualde, Arachidonic-acid-derived eicosanoids: roles in biology and immunopathology. *Trends Mol.Med.* **14**, 461-469 (2008).
22. G. A. Higgs, S. Moncada, J. R. Vane, Eicosanoids in inflammation. *Ann Clin Res* **16**, 287-299 (1984).
23. L. W. Fu, J. C. Longhurst, Bradykinin and thromboxane A2 reciprocally interact to synergistically stimulate cardiac spinal afferents during myocardial ischemia. *Am J Physiol Heart Circ Physiol* **298**, H235-244 (2010).
24. J. C. Longhurst, R. A. Benham, S. V. Rendig, Increased concentration of leukotriene B4 but not thromboxane B2 in intestinal lymph of cats during brief ischemia. *Am J Physiol* **262**, H1482-1485 (1992).

25. S. Zhang, G. Grabauskas, X. Wu, M. K. Joo, A. Heldsinger, I. Song, C. Owyang, S. Yu, Role of prostaglandin D2 in mast cell activation-induced sensitization of esophageal vagal afferents. *Am J Physiol Gastrointest Liver Physiol* **304**, G908-916 (2013).
26. M. S. Gold, L. Zhang, D. L. Wrigley, R. J. Traub, Prostaglandin E(2) modulates TTX-R I(Na) in rat colonic sensory neurons. *J Neurophysiol* **88**, 1512-1522 (2002).
27. C. I. Svensson, M. Zattoni, C. N. Serhan, Lipoxins and aspirin-triggered lipoxin inhibit inflammatory pain processing. *J Exp Med* **204**, 245-252 (2007).
28. M. J. Zylka, F. L. Rice, D. J. Anderson, Topographically distinct epidermal nociceptive circuits revealed by axonal tracers targeted to Mrgprd. *Neuron* **45**, 17-25 (2005).
29. M. W. Buczynski, D. S. Dumlao, E. A. Dennis, Thematic Review Series: Proteomics. An integrated omics analysis of eicosanoid biology. *J Lipid Res* **50**, 1015-1038 (2009).
30. R. R. Ji, Z. Z. Xu, G. Strichartz, C. N. Serhan, Emerging roles of resolvins in the resolution of inflammation and pain. *Trends Neurosci* **34**, 599-609 (2011).
31. A. E. Barden, M. Moghaddami, E. Mas, M. Phillips, L. G. Cleland, T. A. Mori, Specialised pro-resolving mediators of inflammation in inflammatory arthritis. *Prostaglandins Leukot Essent Fatty Acids* **107**, 24-29 (2016).
32. W. S. Powell, J. Rokach, Biosynthesis, biological effects, and receptors of hydroxyeicosatetraenoic acids (HETEs) and oxoeicosatetraenoic acids (oxo-ETEs) derived from arachidonic acid. *Biochim Biophys Acta* **1851**, 340-355 (2015).
33. W. S. Powell, F. Gravelle, S. Gravel, Metabolism of 5(S)-hydroxy-6,8,11,14-eicosatetraenoic acid and other 5(S)-hydroxyeicosanoids by a specific dehydrogenase in human polymorphonuclear leukocytes. *J Biol Chem* **267**, 19233-19241 (1992).
34. W. S. Powell, F. Gravelle, S. Gravel, Phorbol myristate acetate stimulates the formation of 5-oxo-6,8,11,14-eicosatetraenoic acid by human neutrophils by activating NADPH oxidase. *J Biol Chem* **269**, 25373-25380 (1994).
35. Y. Zhang, A. Styhler, W. S. Powell, Synthesis of 5-oxo-6,8,11,14-eicosatetraenoic acid by human monocytes and lymphocytes. *J Leukoc Biol* **59**, 847-854 (1996).
36. U. Zimpfer, S. Dichmann, C. C. Termeer, J. C. Simon, J. M. Schroder, J. Norgauer, Human dendritic cells are a physiological source of the chemotactic arachidonic acid metabolite 5-oxo-eicosatetraenoic acid. *Inflamm Res* **49**, 633-638 (2000).
37. K. R. Erlemann, C. Cossette, S. Gravel, A. Lesimple, G. J. Lee, G. Saha, J. Rokach, W. S. Powell, Airway epithelial cells synthesize the lipid mediator 5-oxo-ETE in response to oxidative stress. *Free Radic Biol Med* **42**, 654-664 (2007).
38. P. B. Stamatiou, C. C. Chan, G. Monneret, D. Ethier, J. Rokach, W. S. Powell, 5-oxo-6,8,11,14-eicosatetraenoic acid stimulates the release of the eosinophil survival factor granulocyte/macrophage colony-stimulating factor from monocytes. *J Biol Chem* **279**, 28159-28164 (2004).
39. M. Guilbert, C. Ferland, M. Bosse, N. Flamand, S. Lavigne, M. Laviolette, 5-Oxo-6,8,11,14-eicosatetraenoic acid induces important eosinophil transmigration through basement membrane components: comparison of normal and asthmatic eosinophils. *Am J Respir Cell Mol Biol* **21**, 97-104 (1999).
40. G. E. Grant, J. Rokach, W. S. Powell, 5-Oxo-ETE and the OXE receptor. *Prostaglandins Other Lipid Mediat* **89**, 98-104 (2009).

41. E. Kocak, E. Akbal, S. Koklu, B. Ergul, M. Can, The Colonic Tissue Levels of TLR2, TLR4 and Nitric Oxide in Patients with Irritable Bowel Syndrome. *Intern Med* **55**, 1043-1048 (2016).
42. T. Shinohara, M. Harada, K. Ogi, M. Maruyama, R. Fujii, H. Tanaka, S. Fukusumi, H. Komatsu, M. Hosoya, Y. Noguchi, T. Watanabe, T. Moriya, Y. Itoh, S. Hinuma, Identification of a G protein-coupled receptor specifically responsive to beta-alanine. *J Biol Chem* **279**, 23559-23564 (2004).
43. D. J. Cavanaugh, H. Lee, L. Lo, S. D. Shields, M. J. Zylka, A. I. Basbaum, D. J. Anderson, Distinct subsets of unmyelinated primary sensory fibers mediate behavioral responses to noxious thermal and mechanical stimuli. *Proc Natl Acad Sci U S A* **106**, 9075-9080 (2009).
44. K. K. Rau, S. L. McIlwrath, H. Wang, J. J. Lawson, M. P. Jankowski, M. J. Zylka, D. J. Anderson, H. R. Koerber, Mrgprd enhances excitability in specific populations of cutaneous murine polymodal nociceptors. *J Neurosci* **29**, 8612-8619 (2009).
45. J. Zhang, D. J. Cavanaugh, M. I. Nemenov, A. I. Basbaum, The modality-specific contribution of peptidergic and non-peptidergic nociceptors is manifest at the level of dorsal horn nociresponsive neurons. *J Physiol* **591**, 1097-1110 (2013).
46. Q. Liu, P. Sikand, C. Ma, Z. Tang, L. Han, Z. Li, S. Sun, R. H. LaMotte, X. Dong, Mechanisms of itch evoked by beta-alanine. *J Neurosci* **32**, 14532-14537 (2012).
47. S. K. Ajit, M. H. Pausch, J. D. Kennedy, E. J. Kaftan, Development of a FLIPR assay for the simultaneous identification of MrgD agonists and antagonists from a single screen. *J Biomed Biotechnol* **2010**, (2010).
48. J. A. Christianson, R. J. Traub, B. M. Davis, Differences in spinal distribution and neurochemical phenotype of colonic afferents in mouse and rat. *J Comp Neurol* **494**, 246-259 (2006).
49. D. R. Robinson, P. A. McNaughton, M. L. Evans, G. A. Hicks, Characterization of the primary spinal afferent innervation of the mouse colon using retrograde labelling. *Neurogastroenterol Motil* **16**, 113-124 (2004).
50. J. R. Hockley, G. Boundouki, V. Cibert-Goton, C. McGuire, P. K. Yip, C. Chan, M. Tranter, J. N. Wood, M. A. Nassar, L. A. Blackshaw, Q. Aziz, G. J. Michael, M. D. Baker, W. J. Winchester, C. H. Knowles, D. C. Bulmer, Multiple roles for NaV1.9 in the activation of visceral afferents by noxious inflammatory, mechanical, and human disease-derived stimuli. *Pain* **155**, 1962-1975 (2014).
51. J. R. F. Hockley, T. S. Taylor, G. Callejo, A. L. Wilbrey, A. Gutteridge, K. Bach, W. J. Winchester, D. C. Bulmer, G. McMurray, E. S. J. Smith, Single-cell RNAseq reveals seven classes of colonic sensory neuron. *Gut*, (2018).
52. R. A. Crozier, S. K. Ajit, E. J. Kaftan, M. H. Pausch, MrgD activation inhibits KCNQ/M-currents and contributes to enhanced neuronal excitability. *J Neurosci* **27**, 4492-4496 (2007).
53. G. Blackburn-Munro, B. S. Jensen, The anticonvulsant retigabine attenuates nociceptive behaviours in rat models of persistent and neuropathic pain. *Eur J Pharmacol* **460**, 109-116 (2003).
54. G. M. Passmore, A. A. Selyanko, M. Mistry, M. Al-Qatari, S. J. Marsh, E. A. Matthews, A. H. Dickenson, T. A. Brown, S. A. Burbidge, M. Main, D. A. Brown, KCNQ/M currents in sensory neurons: significance for pain therapy. *J Neurosci* **23**, 7227-7236 (2003).

55. K. Hirano, K. Kuratani, M. Fujiyoshi, N. Tashiro, E. Hayashi, M. Kinoshita, Kv7.2-7.5 voltage-gated potassium channel (KCNQ2-5) opener, retigabine, reduces capsaicin-induced visceral pain in mice. *Neurosci Lett* **413**, 159-162 (2007).
56. M. Peiris, J. R. Hockley, D. E. Reed, E. S. J. Smith, D. C. Bulmer, L. A. Blackshaw, Peripheral KV7 channels regulate visceral sensory function in mouse and human colon. *Mol Pain* **13**, 1744806917709371 (2017).
57. P. Le Faouder, V. Baillif, I. Spreadbury, J. P. Motta, P. Rousset, G. Chene, C. Guigne, F. Terce, S. Vanner, N. Vergnolle, J. Bertrand-Michel, M. Dubourdeau, N. Cenac, LC-MS/MS method for rapid and concomitant quantification of pro-inflammatory and pro-resolving polyunsaturated fatty acid metabolites. *J Chromatogr B Analyt Technol Biomed Life Sci* **932**, 123-133 (2013).
58. H. Wang, M. J. Zylka, Mrgprd-expressing polymodal nociceptive neurons innervate most known classes of substantia gelatinosa neurons. *J Neurosci* **29**, 13202-13209 (2009).
59. L. Basso, J. Boue, K. Mahiddine, C. Blanpied, S. Robiou-du-Pont, N. Vergnolle, C. Deraison, G. Dietrich, Endogenous analgesia mediated by CD4(+) T lymphocytes is dependent on enkephalins in mice. *J Neuroinflammation* **13**, 132 (2016).
60. J. Boue, L. Basso, N. Cenac, C. Blanpied, M. Rolli-Derkinderen, M. Neunlist, N. Vergnolle, G. Dietrich, Endogenous regulation of visceral pain via production of opioids by colitogenic CD4(+) T cells in mice. *Gastroenterology* **146**, 166-175 (2014).
61. S. M. Brierley, R. C. Jones, 3rd, G. F. Gebhart, L. A. Blackshaw, Splanchnic and pelvic mechanosensory afferents signal different qualities of colonic stimuli in mice. *Gastroenterology* **127**, 166-178 (2004).
62. J. R. Hockley, M. M. Tranter, C. McGuire, G. Boundouki, V. Cibert-Goton, M. A. Thaha, L. A. Blackshaw, G. J. Michael, M. D. Baker, C. H. Knowles, W. J. Winchester, D. C. Bulmer, P2Y Receptors Sensitize Mouse and Human Colonic Nociceptors. *J Neurosci* **36**, 2364-2376 (2016).
63. N. Cenac, M. Castro, C. Desormeaux, P. Colin, M. Sie, M. Ranger, N. Vergnolle, A novel orally administered trimebutine compound (GIC-1001) is anti-nociceptive and features peripheral opioid agonistic activity and Hydrogen Sulphide-releasing capacity in mice. *Eur J Pain* **20**, 723-730 (2016).
64. A. Denadai-Souza, C. M. Ribeiro, C. Rolland, A. Thouard, C. Deraison, C. Scavone, D. Gonzalez-Dunia, N. Vergnolle, M. C. W. Avellar, Effect of tryptase inhibition on joint inflammation: a pharmacological and lentivirus-mediated gene transfer study. *Arthritis Res Ther* **19**, 124 (2017).

Acknowledgments: The authors thank the microscope core facility, INSERM UMR1043, Toulouse; the animal care facility, Genetoul, anexplo, US006/INSERM, Toulouse; and the animal experiment platform of Toxalim (Research Centre in Food Toxicology), Toulouse University, INRA, ENVT, INP-Purpan, UPS, Toulouse, for their technical support. The authors acknowledge the National Diseases Research Interchange (NDRI) for supplying the human DRGs. Lipidomic analyses were performed on the Toulouse INSERM Metatoul-Lipidomique Core Facility-MetaboHub ANR-11-INBS-010. Mrgprd-deficient mice were a generous gift from David J Anderson (Caltech). **Funding:** A.D.-S. was a recipient of a post-doctoral fellowship from São Paulo Research Foundation (FAPESP; process 2012/07784-4). G.B. is a recipient of an educational grant from Fondazione del Monte di Bologna e Ravenna, Bologna, Italy. This work was supported by the Agence Nationale de la Recherche (to N.C.), the Region Midi-Pyrénées (to P.L.F. and N.C.),

the Italian Ministry of Education, University and Research (No. 2002052573 and No. 2007Z292XF and 2009MFSXNZ) and funds from the University of Bologna (to G.B.), funds from Bowel and Cancer Research (to M.M.T.), BBSRC (BB/P007996/1 to D.I.H., and BB/R006210/1 to J.R.F.H and E.S.J.S.), a Rosetrees Postdoctoral Grant (A1296) awarded to J.R.F.H. and E.S.J.S., and a European Research Council (ERC) grant to N.V. (ERC-2012-StG-20111109). This work was also supported by the platform Aninfimip, an EquipEx ('Equipement d'Excellence') supported by the French government through the Investments for the Future program (ANR-11-EQPX-0003). **Author contributions:** T.B., T.P.B., and J.R.F.H. designed research studies, conducted experiments, and acquired and analyzed data. M.M.T., M.R.B., P.L.F., J.P., and C.D. acquired and analyzed data. L.B., C.R., and A.D.S. conducted experiments. A.M., P.M., and D.I.H. raised the different genetically modified mice and participated in the revision of the manuscript. E.J.S. participated in the revision of the manuscript. N.V., A.M., H.E., and G.D. wrote the manuscript. G.B. conducted experiments and wrote the manuscript. D.B. conducted experiments, analyzed data, and wrote the manuscript. N.C. designed research studies, conducted experiments, acquired data, analyzed data, and wrote the manuscript. **Competing interests:** The authors declare that they have no competing interests. **Data and materials availability:** All data needed to evaluate the conclusions in the paper are present in the paper or the Supplementary Materials.

Fig. 1. Quantification of PUFA metabolites in mucosa of IBS patients. (**A**) Heat-map of PUFA metabolites quantified by liquid chromatography-tandem mass spectrometry. Data are shown in a matrix format: each row represents a single PUFA metabolite, and each column represents a subgroup of patients. Each color patch represents the normalized quantity of PUFA metabolites (row) in a subgroup of patients (column), with a continuum of quantity from bright green (lowest) to bright red (highest). The pattern and length of the branches in the dendrograms reflect the relatedness of the PUFA metabolites. The dashed red line is the dendrogram distance used to cluster PUFA metabolites. (**B**) 5-oxoETE quantified by liquid chromatography-tandem mass spectrometry in the mucosa of HCs (white circle) and patients with the indicated type of IBS (black circle). Data are expressed in pg/mg protein and presented as means ± SEM of 10 to 20 biopsies per group. Statistical analysis was performed using Kruskal-Wallis analysis of variance and subsequent Dunn's post hoc test. ***$P < 0.001$ compared to the HC group.

Fig. 2. 5-oxoETE induces somatic and visceral hypersensitivity in vivo. (**A** to **E**) Eight-week-

old male C57BL/6J mice were subcutaneously injected with either HBSS (white circle) or 5-oxoETE (black circle) into hind footpads. (A) Somatic pain was monitored using the von Frey test at the indicated times after injection with 10 μM 5-oxoETE or HBSS. Data are means of three independent experiments with 5 mice per group. Errors bars indicate SEM. (B) The Von Frey test was performed 30 min after injection of the indicated concentrations of 5-oxoETE. Data are means ± SEM of two experiments with six mice per group. (C) Mouse paw tissue samples were stained with H&E 6 hours after the administration of HBSS or 100 μM 5-oxoETE as indicated. Images are representative of two experiments with 5 mice per group. (D) Visceromotor response (VMR) to increasing pressures of colorectal distension before and 30 min after intracolonic administration of 10μM 5-oxoETE (black bars) or vehicle (40% ethanol; white bars). Data are means ± SEM of two experiments with 10 mice per group and are relative to the baseline recorded before treatment. (E) Colon tissue samples stained with H&E from mice treated with 40% ethanol or 10 μM 5-oxoETE as indicated. Images are representative of two experiments with 5 mice per group. Statistical analysis was performed using Kruskal-Wallis analysis of variance and subsequent Dunn's post hoc test. $^{**}P < 0.01$, $^{***}P < 0.001$, compared to control mice.

Fig. 3. 5-oxoETE induces lumbar splanchnic nerve firing. (**A**) Example of a teased-fiber recording showing the lumbar splanchnic (that is, colon-innervating) nerve response to ring application (7 min) of 5-oxoETE in mouse serosal afferents. Arrows indicate application and removal of 5-oxoETE. Data are representative of eight experiments in which 5-oxoETE elicited nerve discharge above baseline from a total of 21 teased fibers isolated from 7 mice. (**B**) Mean change in firing/s in serosal receptive fields in response to 5-oxo-ETE compared with the response to vehicle (Krebs buffer). Data are means ± SEM of 8 teased-fiber recordings (N = 7 mice) for 5-

oxoETE and 5 teased-fiber recordings (N = 5 mice) for vehicle. Statistical analysis was performed using a Mann-Whitney t-test. $^{**}P < 0.01$ compared to vehicle. (**C**) Proportion of responses in lumbar splanchnic afferents to application of 5-oxoETE (n, number of teased-fiber recordings; N, number of mice).

Fig. 4. 5-oxoETE induces an increase in $[Ca^{2+}]_i$ in sensory neurons through a GPCR. (**A**) Representative trace of Ca^{2+} flux experiments in sensory neurons incubated in the absence of extracellular Ca^{2+}/Mg^{2+} and exposed to 50 μM 5-oxoETE or vehicle (HBSS). (**B**) Ca^{2+} flux measurements in mouse sensory neurons exposed to the indicated concentrations of 5-oxoETE (black circle) or to vehicle (HBSS; white circle). Data are means + SEM of seven independent experiments with 3 wells per condition and 60 to 80 neurons per well. (**C**) Amplitude of $[Ca^{2+}]_i$ (ΔF/F; left) in human sensory neurons and the percentage of responding neurons (right) exposed to the indicated concentrations of 5-oxoETE (black bar) or to vehicle (HBSS; white bar). Data are means ± SEM of three independent experiments with 3 wells per condition and 20 to 53 neurons per well. (**D**) Percentages of isolectin B4–positive ($IB4^+$) and IB4-negative ($IB4^-$) mouse sensory neurons that responded to 10 μM 5-oxoETE (black bars) or HBSS (white bars). Data are means ± SEM of three independent experiments with 3 wells per condition and 60 to 80 neurons per well. (**E**) Effects of 30-min incubation with 10 μM U73122 (PLC inhibitor) or overnight incubation with PTX (250 ng/ml) on 5-oxoETE–induced Ca^{2+} mobilization in mouse sensory neurons. Data are means ± SEM of five independent experiments with 3 wells per condition and 60 to 80 neurons per well. Statistical analysis was performed using Kruskal-Wallis analysis of variance and subsequent Dunn's post hoc test. $^{*}P < 0.05$, $^{**}P < 0.01$, $^{***}P < 0.001$ compared to HBSS.

Fig. 5. Expression of *Mrgprd* in sensory neurons. (**A**) Expression of *Mrgprd* (red) and *Trpv1* (blue) mRNA transcripts as detected by single-cell qRT-PCR analysis (middle) of retrogradely labelled mouse colonic sensory neurons (left). Pie chart representation (right) of the expression (dark color) or not (light color) of *Mrgprd* and *Trpv1* mRNA in Fast Blue (FB)-positive neurons. Each segment represents a single colonic sensory neuron. (**B**) Representative images of GFP (green), CGRP-immunoreactivity (red), and FB labelling (blue) in a T13 DRG from a $Mrgprd^{EGFP}$ mouse in which FB was injected into the colon. Scale bar, 50 µm. Inset images are magnifications of the boxed areas in the largest images. (**C** and **D**) Expression of Mrgprd by immunostaining in a whole human T11 DRG (C) and in a primary culture of human sensory neurons using confocal microscopy (D). Pie chart representation of the immunoreactivity (dark color) or not (light color) of Mrgprd in Pgp9.5-positive neurons. Each segment represents a single sensory neuron. Scale bars, 10 µm. Images are representative of 2 experiments with 10 slides per experiment (C) and of 5 experiments with 2 wells per experiment (D).

Fig. 6. Mrgprd expression is required for the intracellular Ca^{2+} mobilization and hypersensitivity induced by 5-oxoETE. (**A**) Left: Representative image of sensory neurons transfected with shRNA (red) and containing the Ca^{2+} indicator Fluo4 (green). Right: Percentage of sensory neurons expressing control shRNA or *Mrgprd*-specific shRNA that responded to HBSS or 10 µM 5-oxoETE. Data are means ± SEM of six independent experiments with 3 wells per conditions and 10 to 32 analyzed neurons per well. (**B**) Percentage of responding neurons (left) and amplitude of intracellular Ca^{2+} mobilization (ΔF/F; right) in mouse sensory neurons from Mrgprd-deficient mice exposed to vehicle (HBSS; white bar), 10 µM 5-oxoETE (black bar), or to a mixture of GPCR agonists (GPCR Mix: bradykinin, serotonin, and histamine, 10 µM each; gray

bar). Data are means ± SEM of four independent experiments with 3 wells per condition and 20 to 50 neurons per well. (**C**) Effects of the indicated concentrations of 5-oxoETE and of 1 mM β-alanine (positive control) on the amplitude (ΔF/F) of Ca^{2+} mobilization in HEK cells transiently transfected with plasmid expressing *Mrgprd* or with an empty vector as a control. Data are means ± SEM of eight independent experiments with 3 wells per condition. (**D**) Visceromotor response (VMR) in Mrgprd-deficient mice in response to increasing pressures of colorectal distension before (baseline; white circle) and 30 min after intracolonic administration of 10 µM 5-oxoETE (black circle). Data are means + SEM of two experiments of 7 mice per experiment. Statistical analysis was performed using Kruskal-Wallis analysis of variance and subsequent Dunn's post hoc test. In (A), $^{**}P < 0.01$ compared to the control shRNA/HBSS group; In (B), $^{**}P < 0.01$ compared to the HBSS group; In (C), $^{*}P < 0.05$, $^{**}P < 0.01$, $^{***}P < 0.001$ compared to the corresponding CHO empty vector group.

Table 1. Characteristics of patients from which biopsies were collected for the quantification of PUFA metabolites.

	Control	**IBS**
Number	14	50
Age	49 (20-76)	43 (20-72)
Sex ratio (F/M)	8/6	32/18
Bowel movements:		
Diarrhea	0	20
Constipation	0	20
Mix	0	10

Table 2. Percentage of Fast Blue–positive neurons expressing Mrgprd, CGRP, or both in T13 DRGs per *Mrgprd*^{EGFP} mouse.

Animal	Mrgprd^{+}	CGRP^{+}	Mrgprd^{+} and CGRP^{+}
A	9 / 75 (12.0%)	54 / 75 (72.0%)	0 / 75 (0.0%)
B	2 / 38 (5.3%)	24 / 38 (63.2%)	0 / 38 (0.0%)
C	10 / 101 (9.9%)	64 / 101 (63.4%)	1 / 101 (1.0%)
D	1 / 60 (1.7%)	46 / 60 (76.7%)	0 / 60 (0.0%)
Total (mean ± SD)	7.2 ± 4.6 %	68.8 ± 6.7 %	0.3 ± 0.5 %

Figure 1

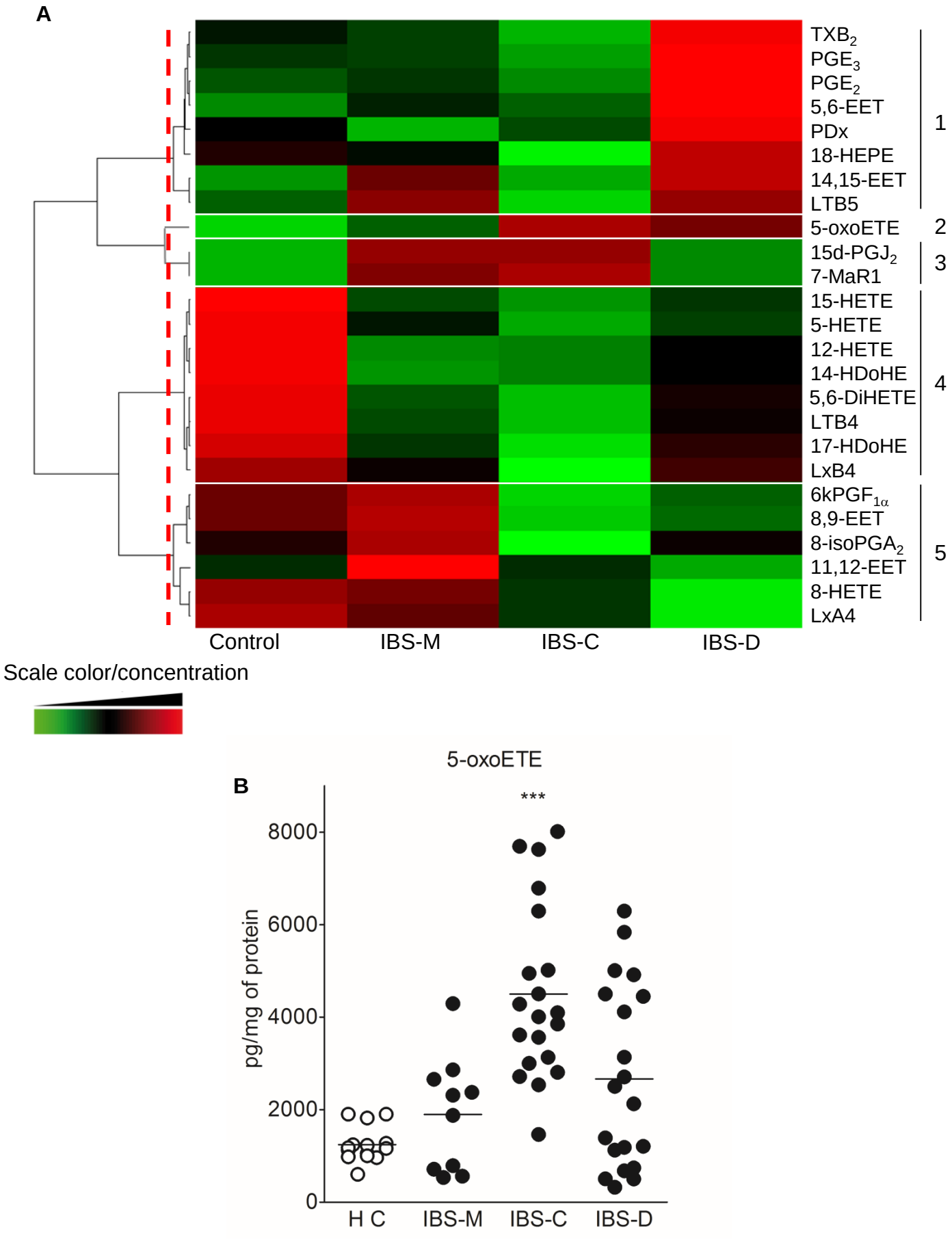
A
TXB2
PGE3
PGE2
5,6-EET
PDx
18-HEPE
14,15-EET
LTB5
5-oxoETE
15d-PGJ2
7-MaR1
15-HETE
5-HETE
12-HETE
14-HDoHE
5,6-DiHETE
LTB4
17-HDoHE
LxB4
6kPGF1α
8,9-EET
8-isoPGA2
11,12-EET
8-HETE
LxA4
1
2
3
4
5
Control
IBS-M
IBS-C
IBS-D
Scale color/concentration
B
5-oxoETE
***
pg/mg of protein
8000
6000
4000
2000
0
H C
IBS-M
IBS-C
IBS-D

Figure 2

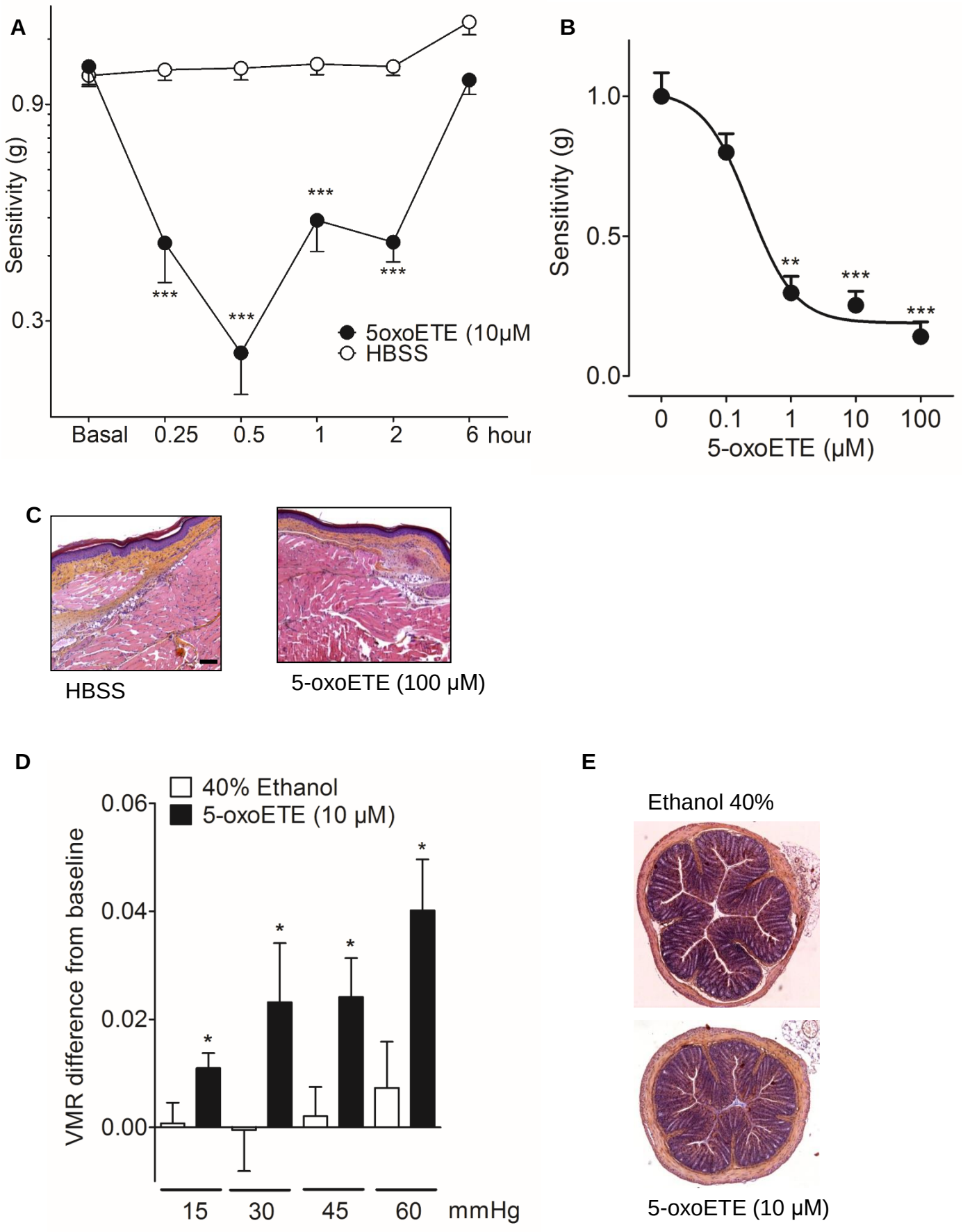
A
Sensitivity (g)
0.9
0.3
***
***
***
***
5oxoETE (10μM
HBSS
Basal
0.25
0.5
1
2
6 hour
B
Sensitivity (g)
1.0
0.5
0.0
**
***
***
0
0.1
1
10
100
5-oxoETE (μM)
C
HBSS
5-oxoETE (100 μM)
D
40% Ethanol
5-oxoETE (10 μM)
VMR difference from baseline
0.06
0.04
0.02
0.00
*
*
*
*
15
30
45
60
mmHg
E
Ethanol 40%
5-oxoETE (10 μM)

Figure 3

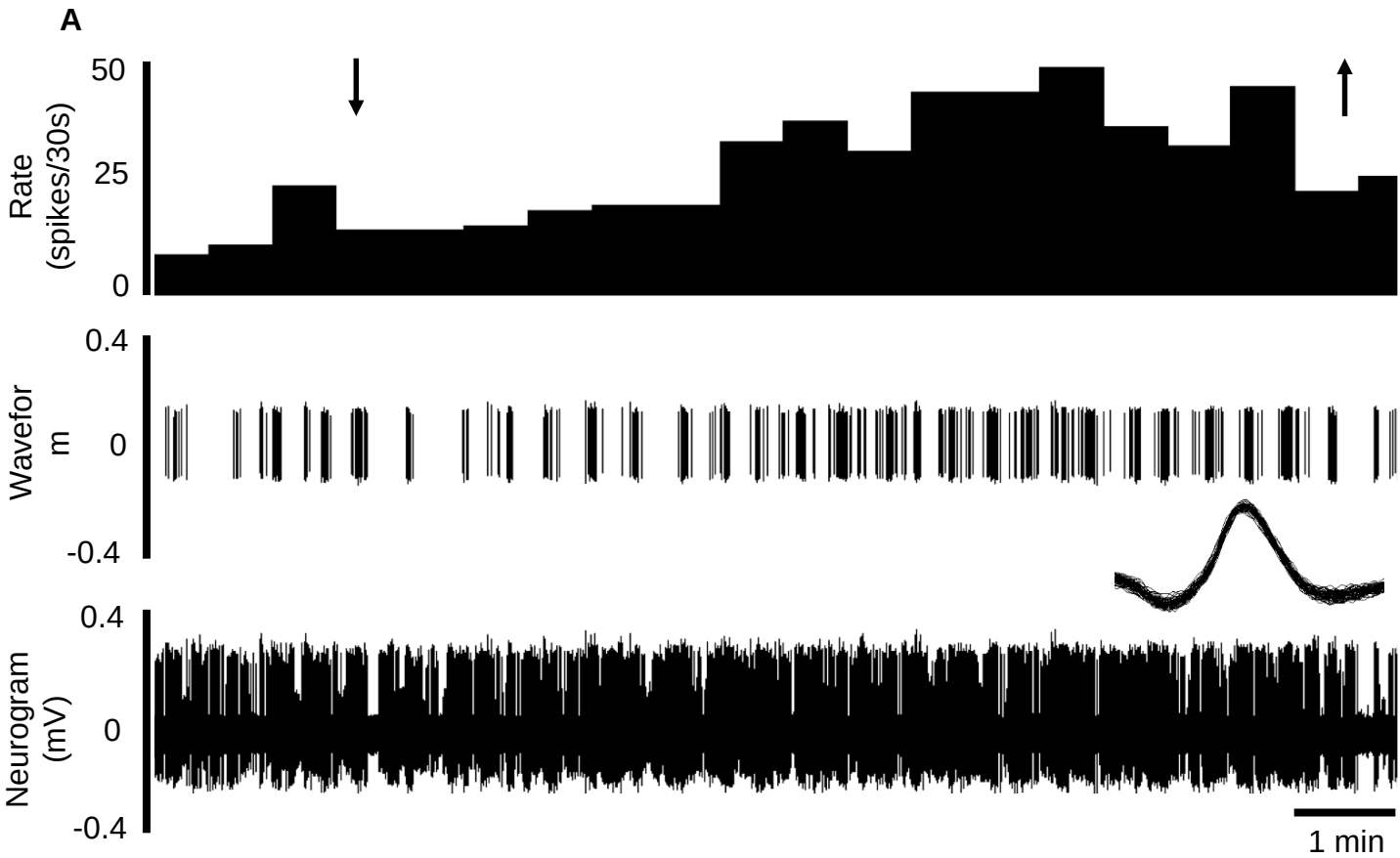
A
Rate (spikes/30s)
50
25
0
Wavefor m
0.4
0
-0.4
Neurogram (mV)
0.4
0
-0.4
1 min

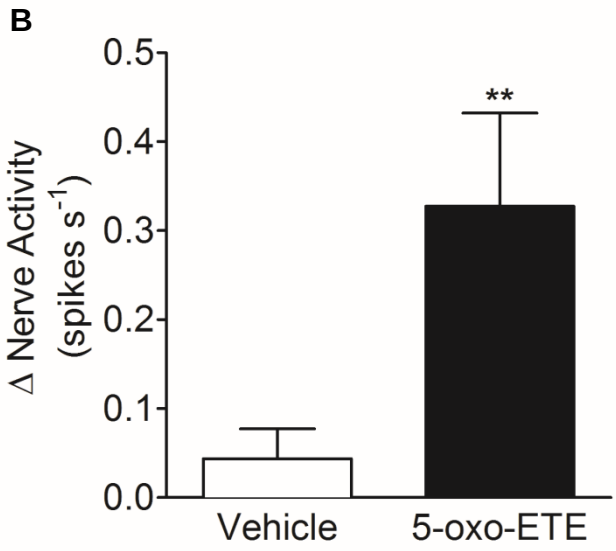
B
Δ Nerve Activity (spikes s-1)
0.5
0.4
0.3
0.2
0.1
0.0
**
Vehicle
5-oxo-ETE

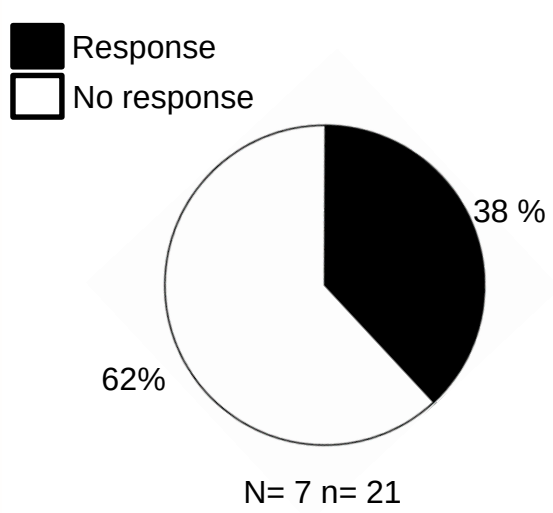
C
Response
No response
38 %
62%
N= 7 n= 21

Figure 4

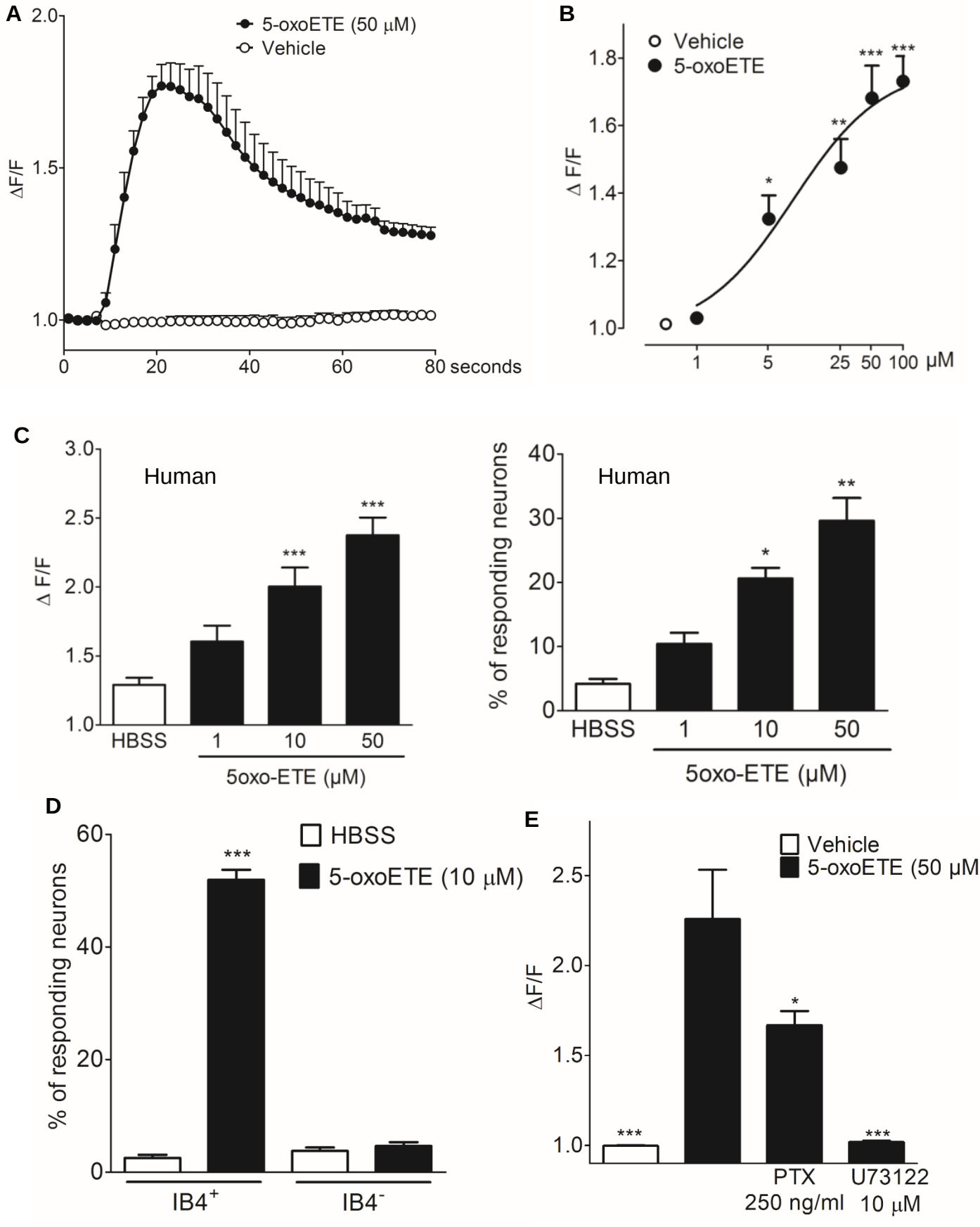
A
5-oxoETE (50 μM)
Vehicle
ΔF/F
2.0
1.5
1.0
0
20
40
60
80 seconds
B
Vehicle
5-oxoETE
Δ F/F
1.8
1.6
1.4
1.2
1.0
*
**
***
***
1
5
25
50
100 μM
C
Human
Δ F/F
3.0
2.5
2.0
1.5
1.0
***
***
HBSS
1
10
50
5oxo-ETE (μM)
Human
% of responding neurons
40
30
20
10
0
*
**
HBSS
1
10
50
5oxo-ETE (μM)
D
% of responding neurons
60
40
20
0
***
HBSS
5-oxoETE (10 μM)
IB4+
IB4-
E
Vehicle
5-oxoETE (50 μM)
ΔF/F
2.5
2.0
1.5
1.0
***
*
***
PTX
250 ng/ml
U73122
10 μM

Figure 5

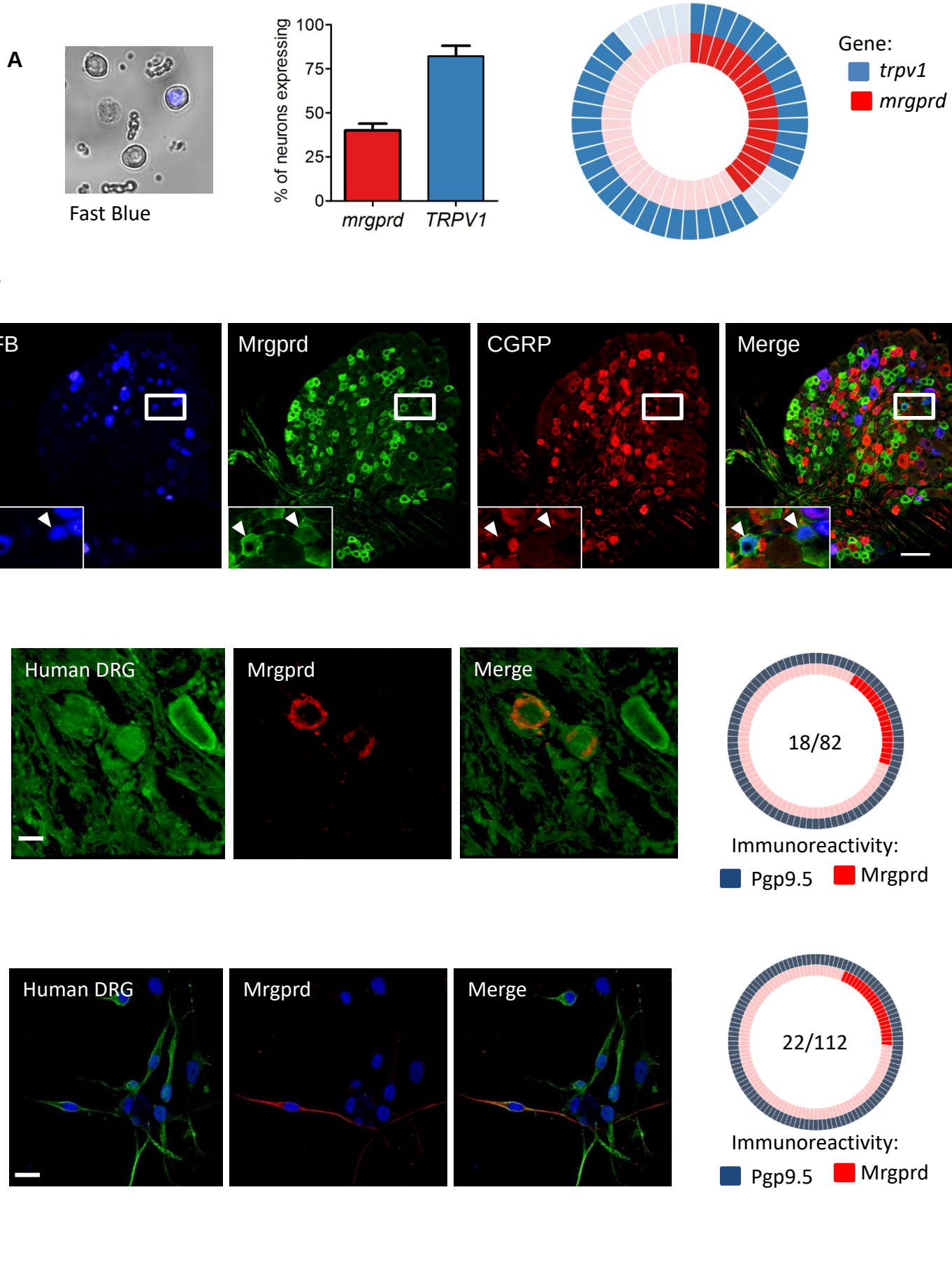
A
Fast Blue
% of neurons expressing
100
75
50
25
0
mrgprd
TRPV1
Gene:
trpv1
mrgprd
B
FB
Mrgprd
CGRP
Merge
C
Human DRG
Mrgprd
Merge
18/82
Immunoreactivity:
Pgp9.5
Mrgprd
D
Human DRG
Mrgprd
Merge
22/112
Immunoreactivity:
Pgp9.5
Mrgprd

Figure 6

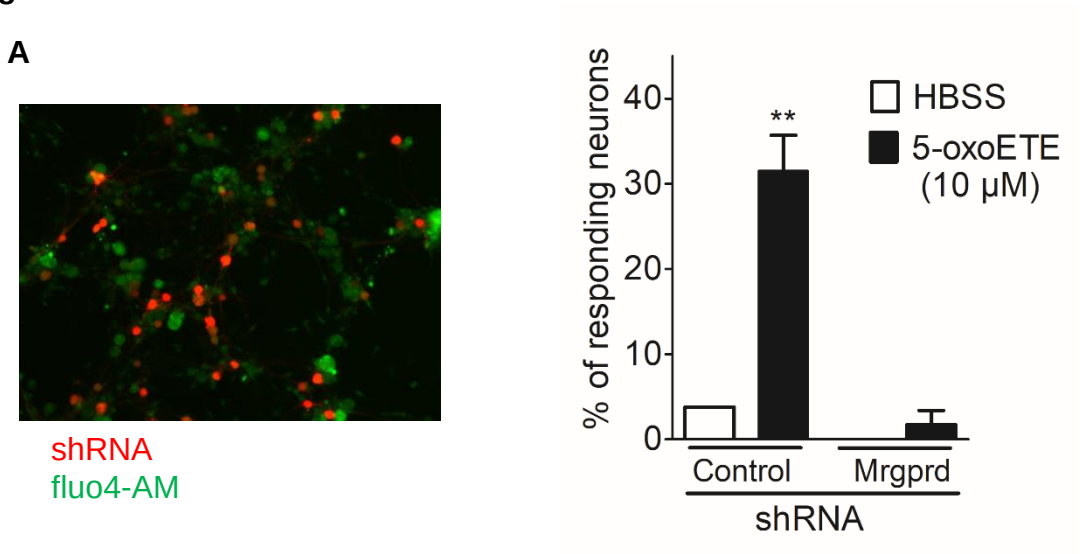
A
shRNA
fluo4-AM
% of responding neurons
HBSS
5-oxoETE
(10 μM)
Control
Mrgprd
shRNA
B
% Responding neurons
HBSS
GPCR Mix
5-oxoETE
ΔF/F
C
CHO Mrgprd
CHO empty vector
5-oxoETE
β-Alanine
μM
D
Baseline
5-oxoETE (10 μM)
VMR (mv/s)
mmHg